Challenges of Applying Ground Motion Simulation to Earthquake Engineering

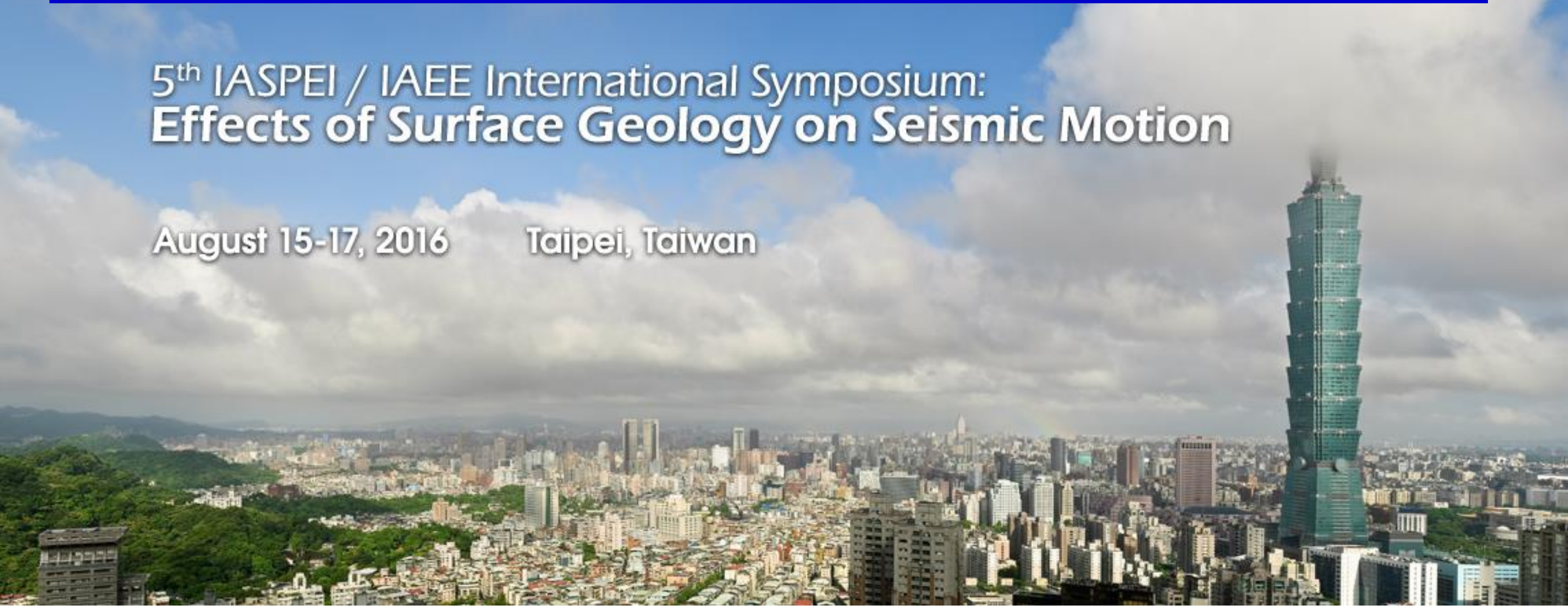

Methodology of simulating ground motions from crustal earthquake and mega-thrust subduction earthquakes: application to the 2016 Kumamoto earthquake (crustal) and the 2011 Tohoku earthquake (mega-thrust)

Kojiro Irikura[1], Ken Miyakoshi[2] and Susumu Kurahashi[1]

1) Aichi Institute of Technology, 2) Geo-Research Institute

Presentation content

1. Methodology of simulating ground motions from crustal earthquakes
1.1. Recipe of strong motion prediction for crustal earthquakes
1.2 Scaling relationships of source parameters for crustal earthquake
1.3 Simulation of strong ground motion following the recipe for crustal earthquake

2. Methodology of simulating ground motions from mega-thrust subduction earthquakes
2.1. Dynamic source model with a multi-scale heterogeneity
2.2. Scaling relationships of source parameters for mega-thrust subduction earthquakes
2.3. Simulation of strong ground motion following the recipe for crustal earthquake

3. Summary

Source Characterization for Simulating Strong Ground Motion

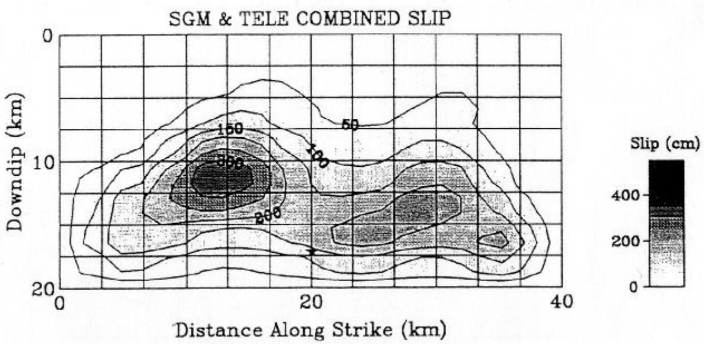

Wald et al. (1991)

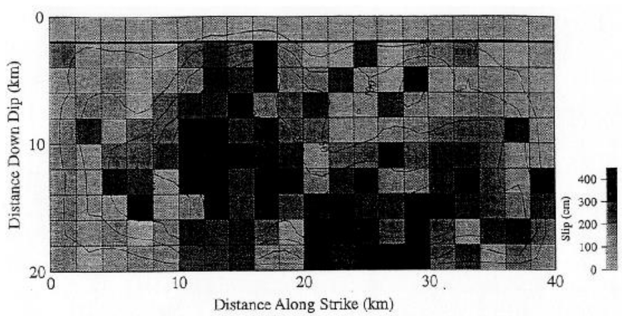

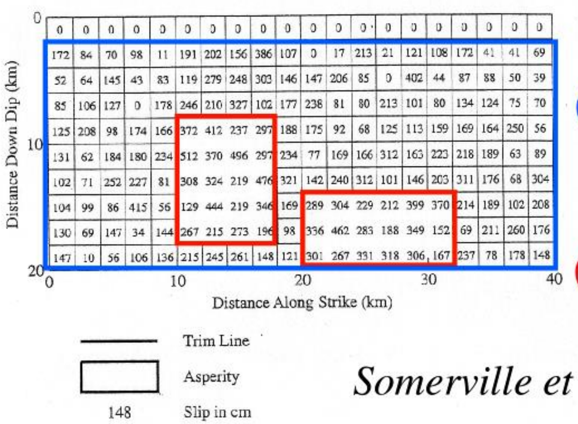

rupture area ($>= 0.3\Delta\bar{D}_{total}$)

asperity ($>=1.5\Delta\bar{D}_{rup}$)

Somerville et al. (1999)

1989 Loma Prieta earthquake (M_w6.9)

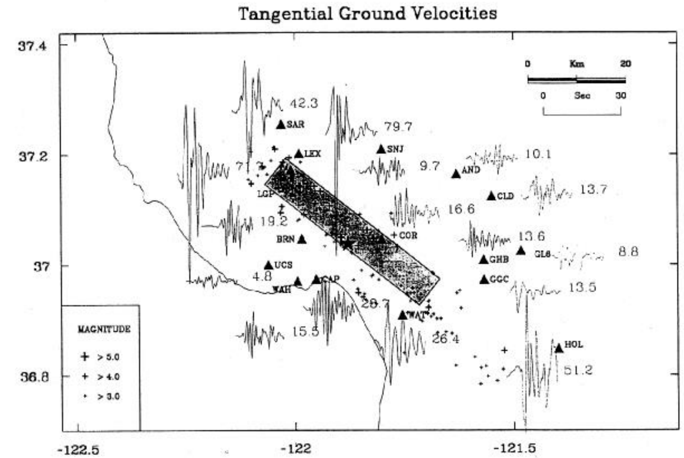

effective source dimension

(L_{eff}, W_{eff} are derived by auto-correlation of slip distribution)

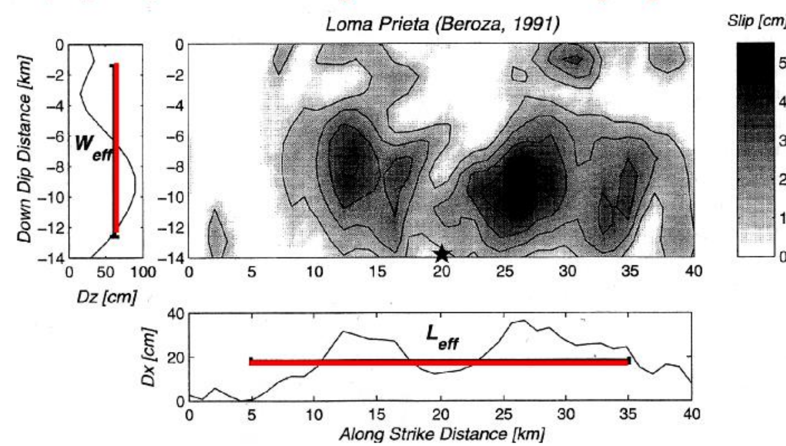

Mai and Beroza (2000)

Illustration of Characterized Source Model

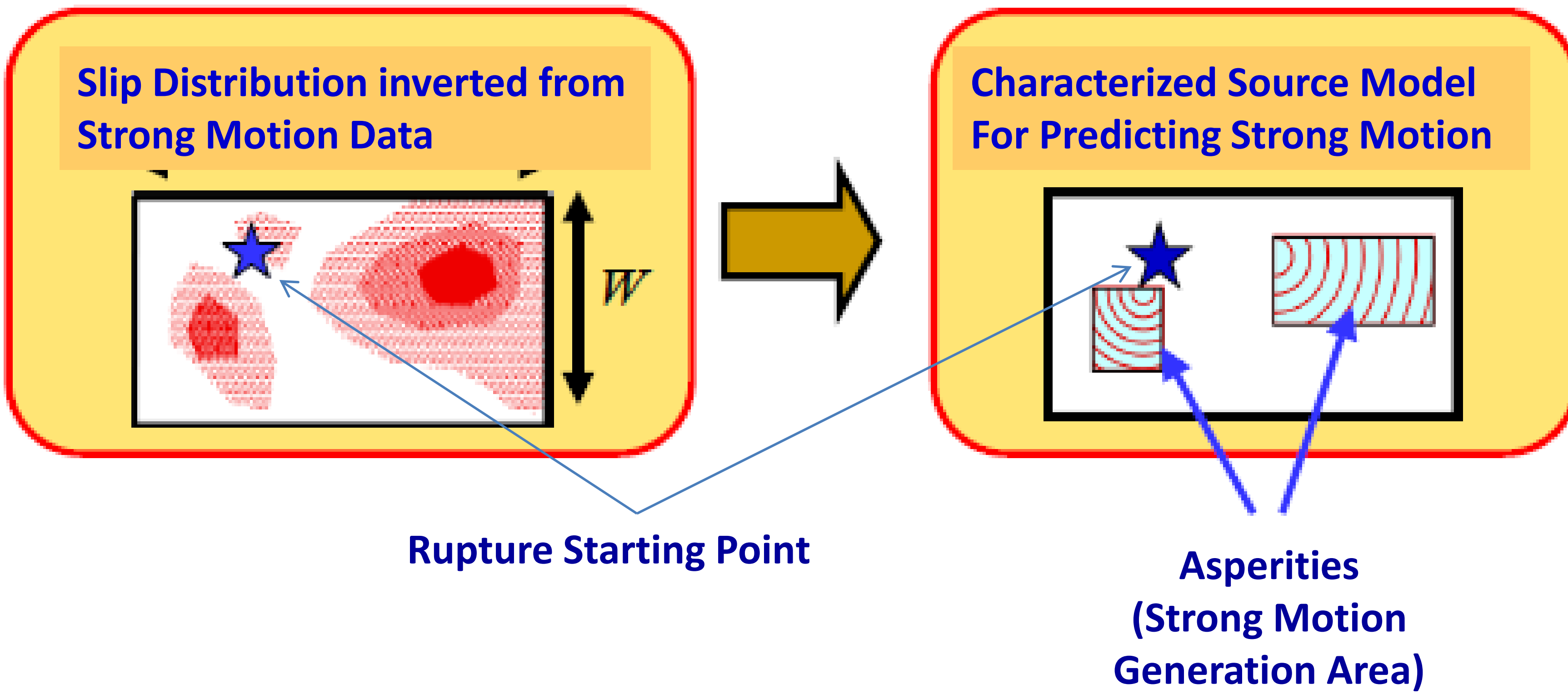

Recipe of predicting strong ground motions for crustal earthquakes

1. Estimation of source area of crustal earthquake

   Entire rupture area

   → Total seismic moment and average stress drop

   → Outer fault parameters

2. Heterogeneity (Roughness) of stress drop inside source area

   Asperities (Strong motion generation area)

   → Combined area of asperities and stress drop on the asperities

   → Inner fault parameters

3. Extra important parameters

   Rupture starting point,

   Rupture propagation pattern, Rupture velocity

Validation of the Recipe for the Mw 7.0 2016 Kumamoto Earthquakes

Scaling Relationships of outer and inter source parameters

Relationship between rupture area and seismic moment
Relationship between combined area of asperities and rupture area
Stress parameters of asperities

Simulation of ground motions using the characterized source model based on the recipe

Two source models are tested.

1. Three-segments model
2. Single-segment model

Simulated motions based on the recipe are compared with observed records from the Mw 7.0 2016 Kumamoto Earthquakes

Map View of the 2016 Kumamoto earthquake (Mw 7.0)

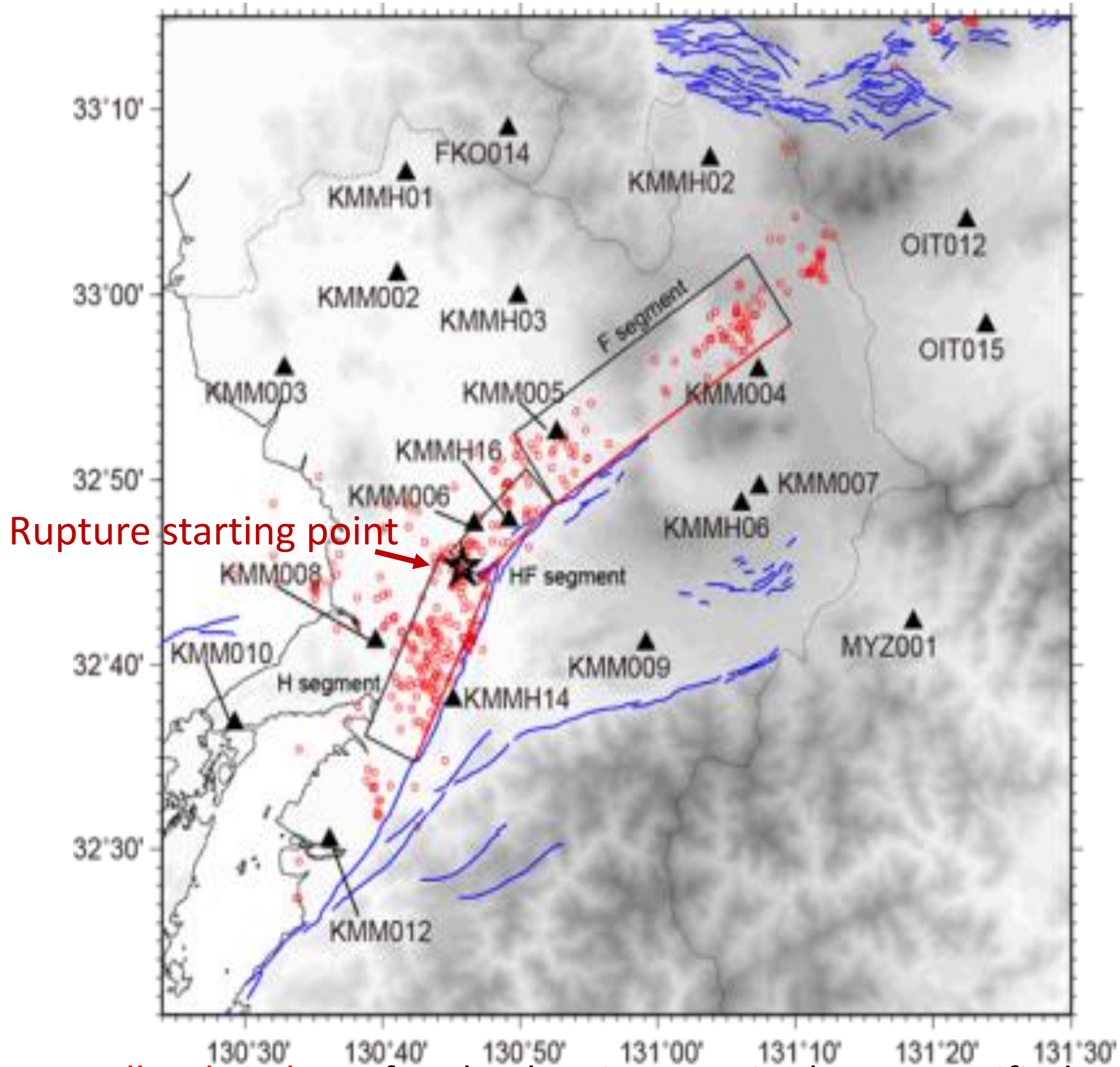

Small red circles: Aftershock epicenters in the JMA unified catalog first 48 hours after the mainshock.

Slip Distribution of the Mw 7.0 2016 Kumamoto Earthquake

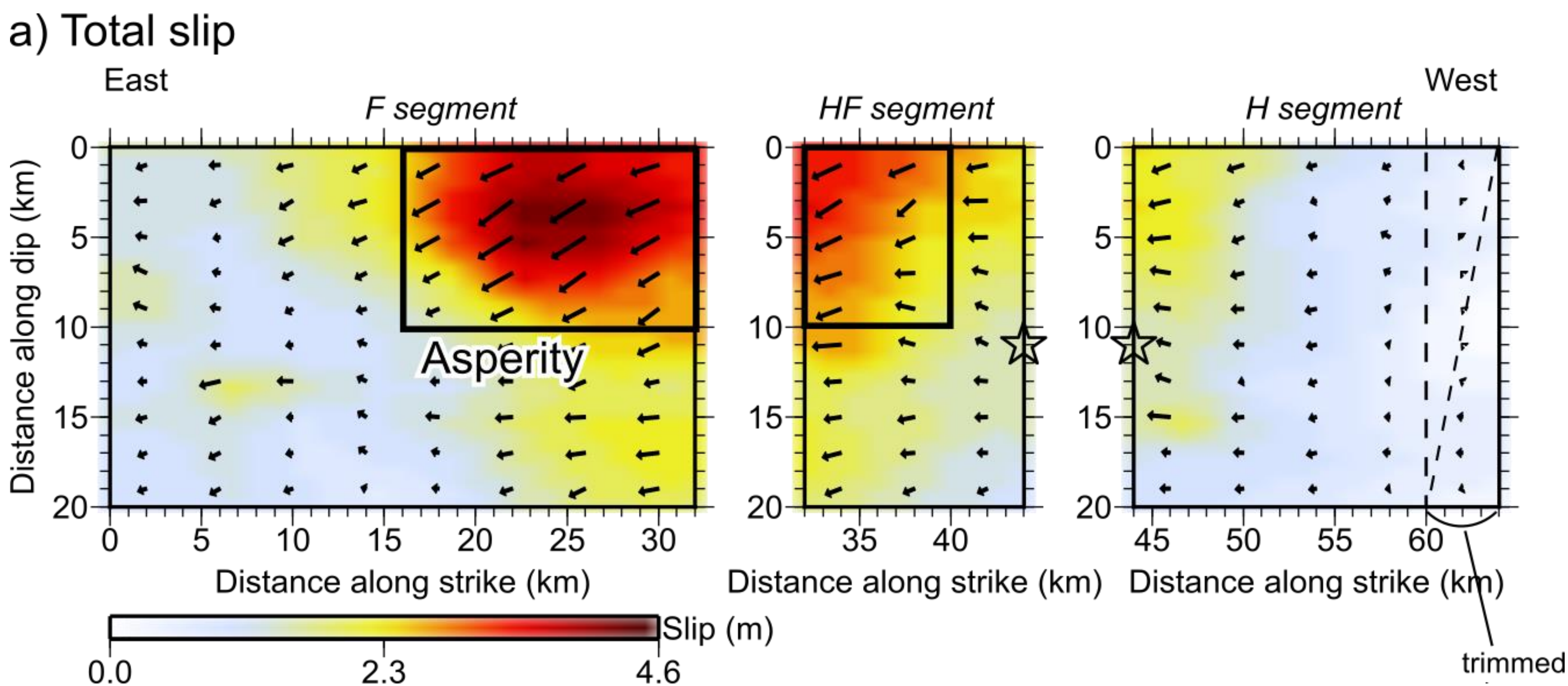

Relationship between Rupture area and Seismic Moment

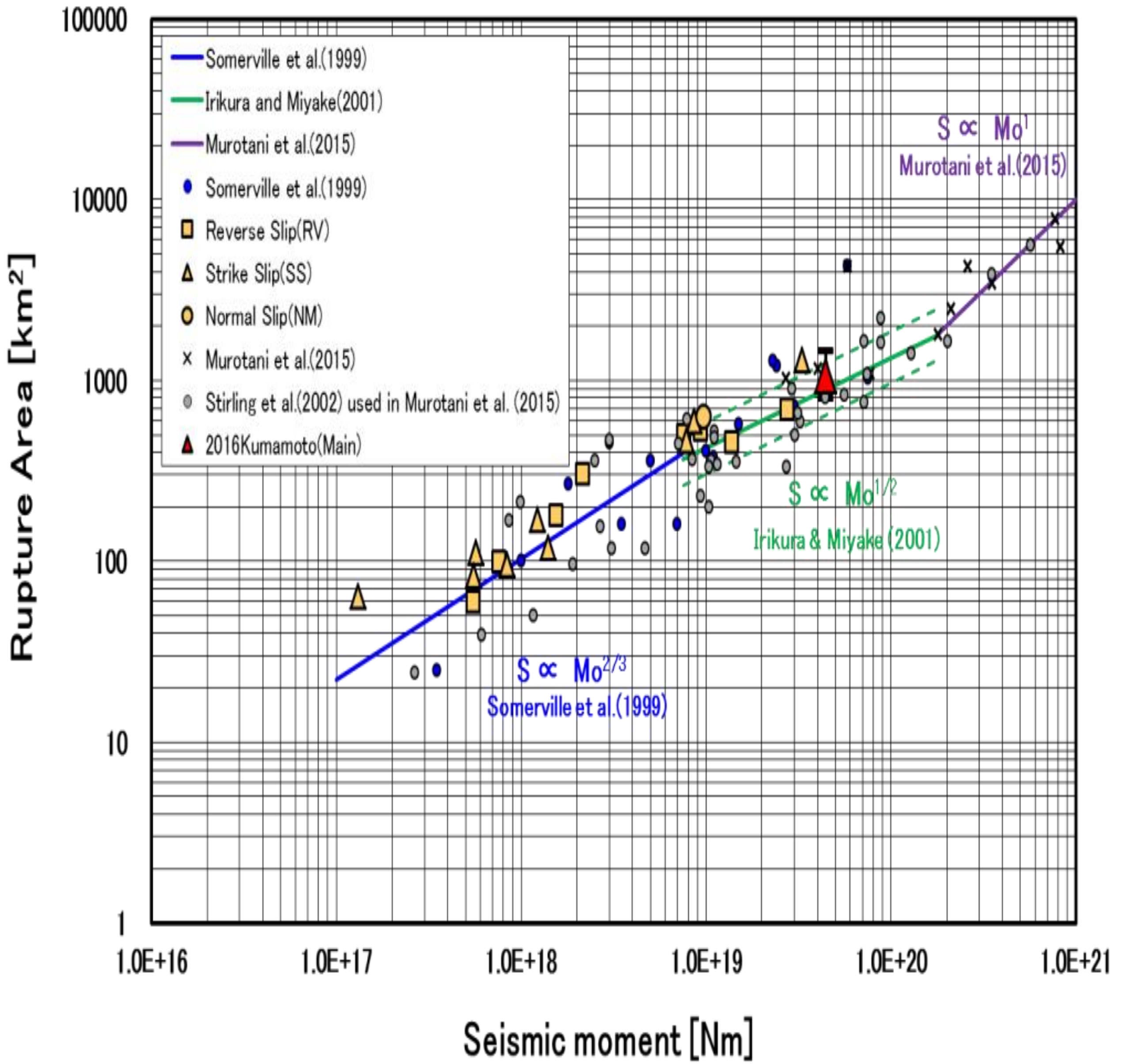

Red Triangle: the Mw 7.0 Kumamoto earthquake

Relationship between Average Slip and Seismic Moment

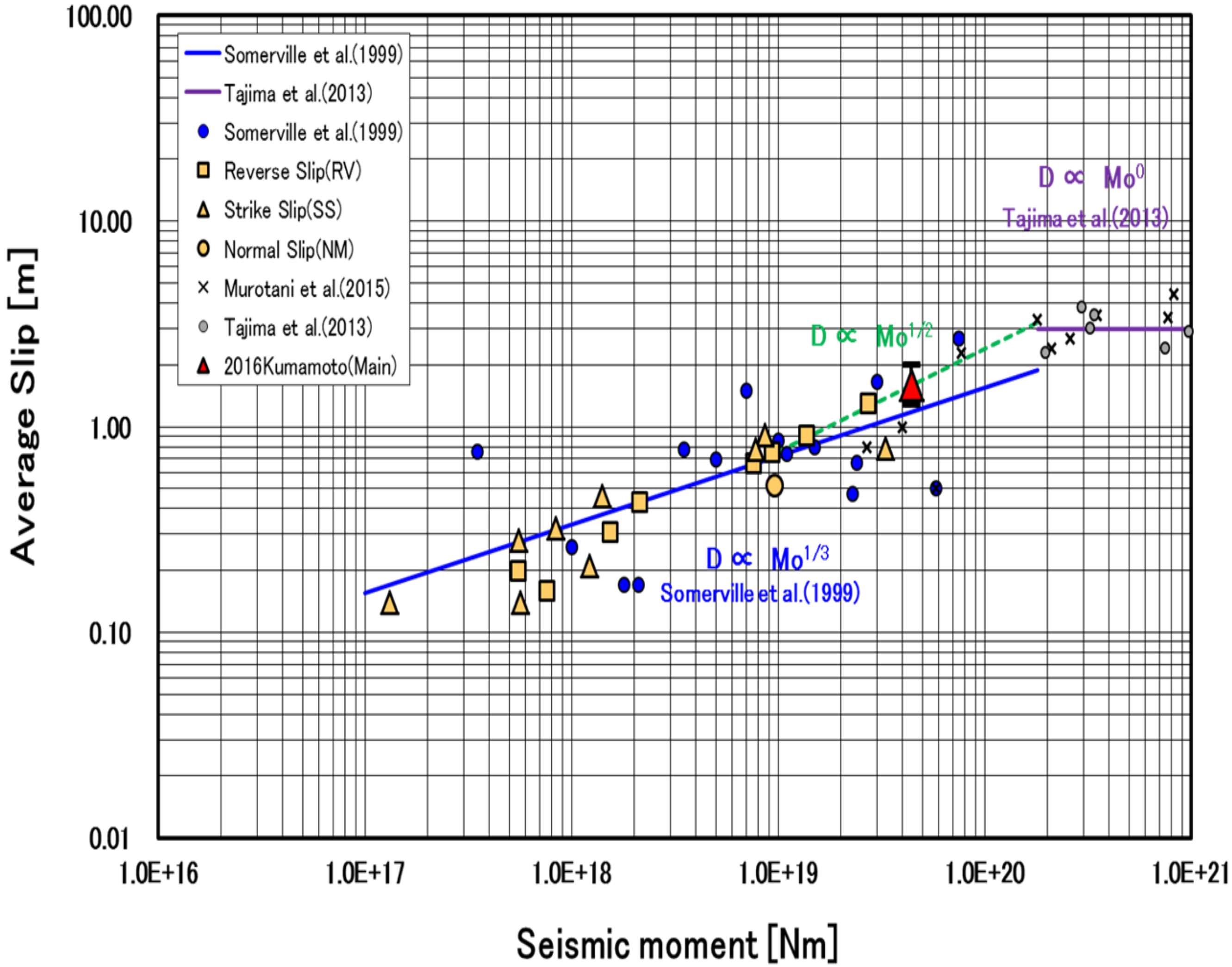

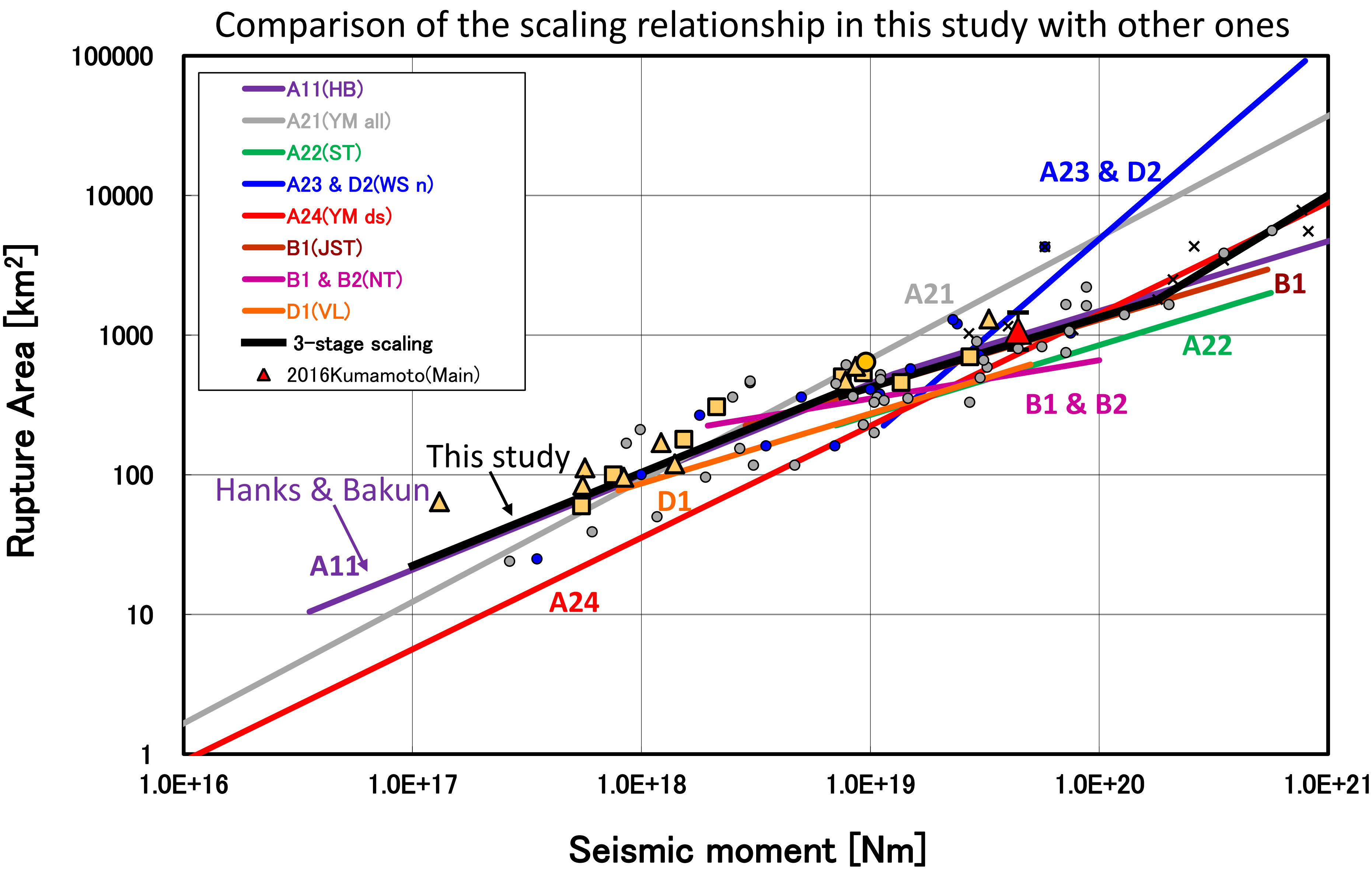

Fig.4(b) Three stage scaling model (black solid line) in comparison with regressions of Mo – S (rupture area) compiled by Stirling et al. (2013).

*Identifiers (A, B, and D) in the legend correspond to the tectonic regime classification by Stirling et al. (2013).
A, Plate boundary crustal ; B, Stable continental ; and D, Volcanic

*Abbreviation in parentheses refer to authors of the regressions: HB, Hanks and Bakun (2008) ; YM, Yen and Ma (2011) ; ST, Stirling et al. (2008) ; WS, Wesnousky (2008) ; NT, Nuttli (1983) ; JST, Johnston (1994); and VL, Villamor et al. (2001).

*Slip types : all, all slip ; n, normal slip ; ds, dip slip.

Selection of Mw 4.9 event records as the empirical Green's functions

Subfault area is estimated from the corner frequency of the Mw 4.9.

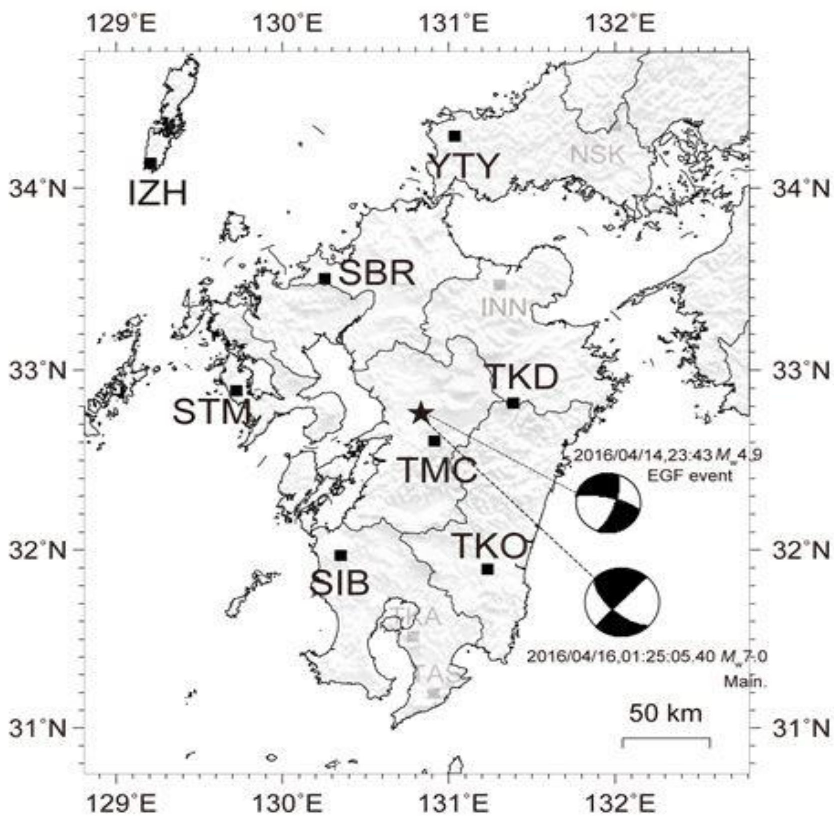

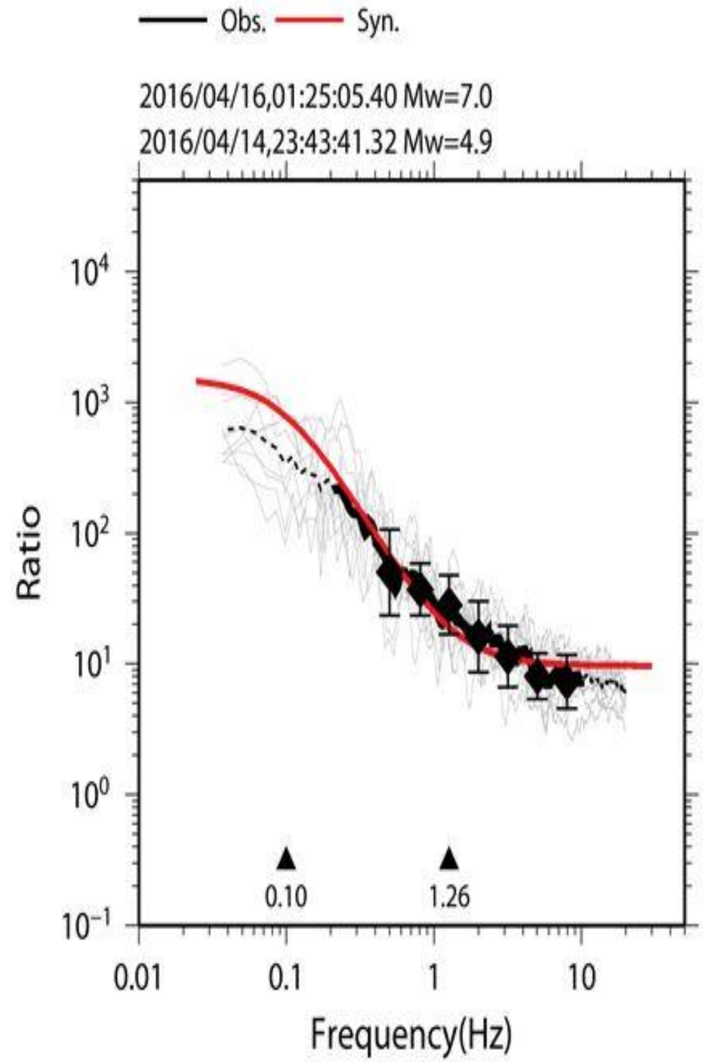

Best-fit characterized source model with three SMGAs based on the inversion result by Yoshida et al. (2016)

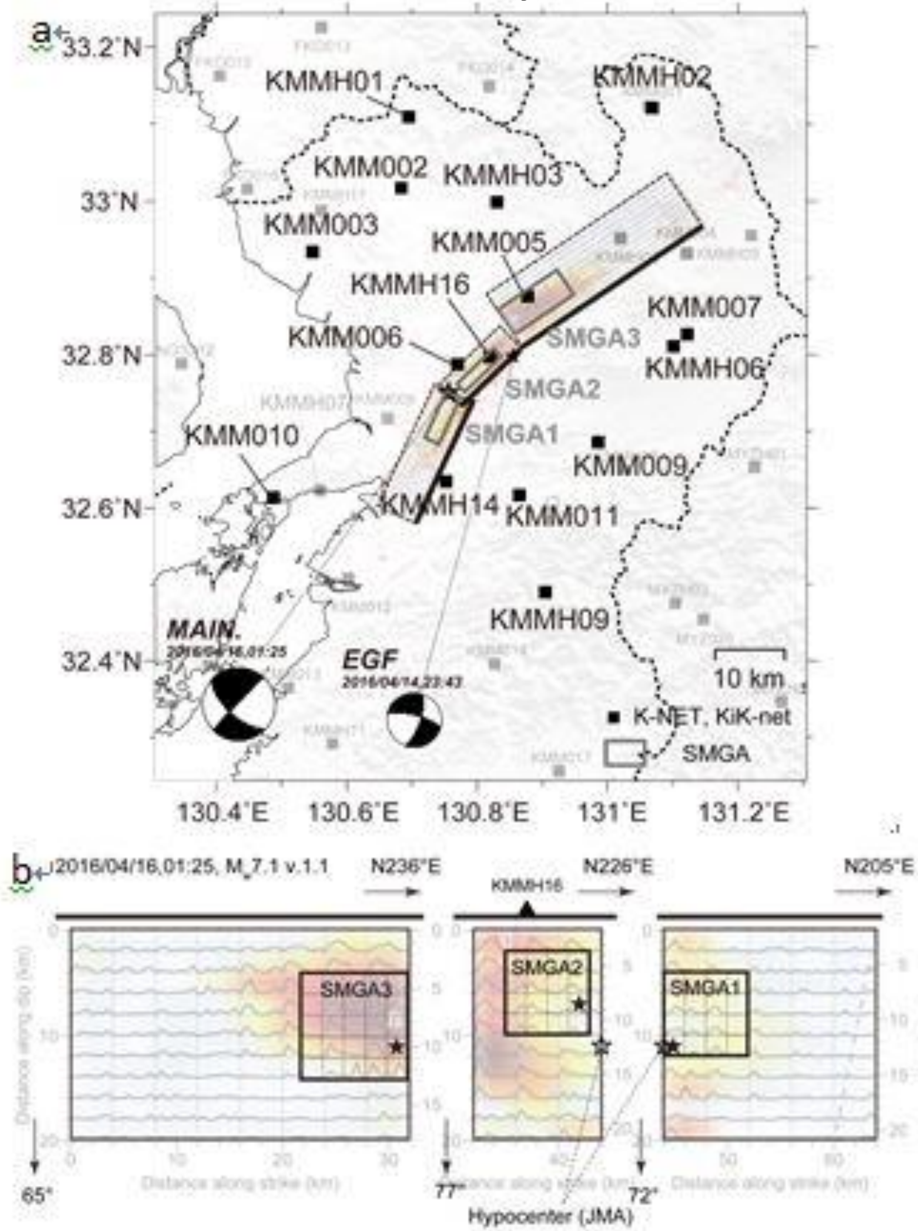

Comparison between observed and synthetic ground motions for three-SMGAs model

Black - observed
Red - Synthetic.

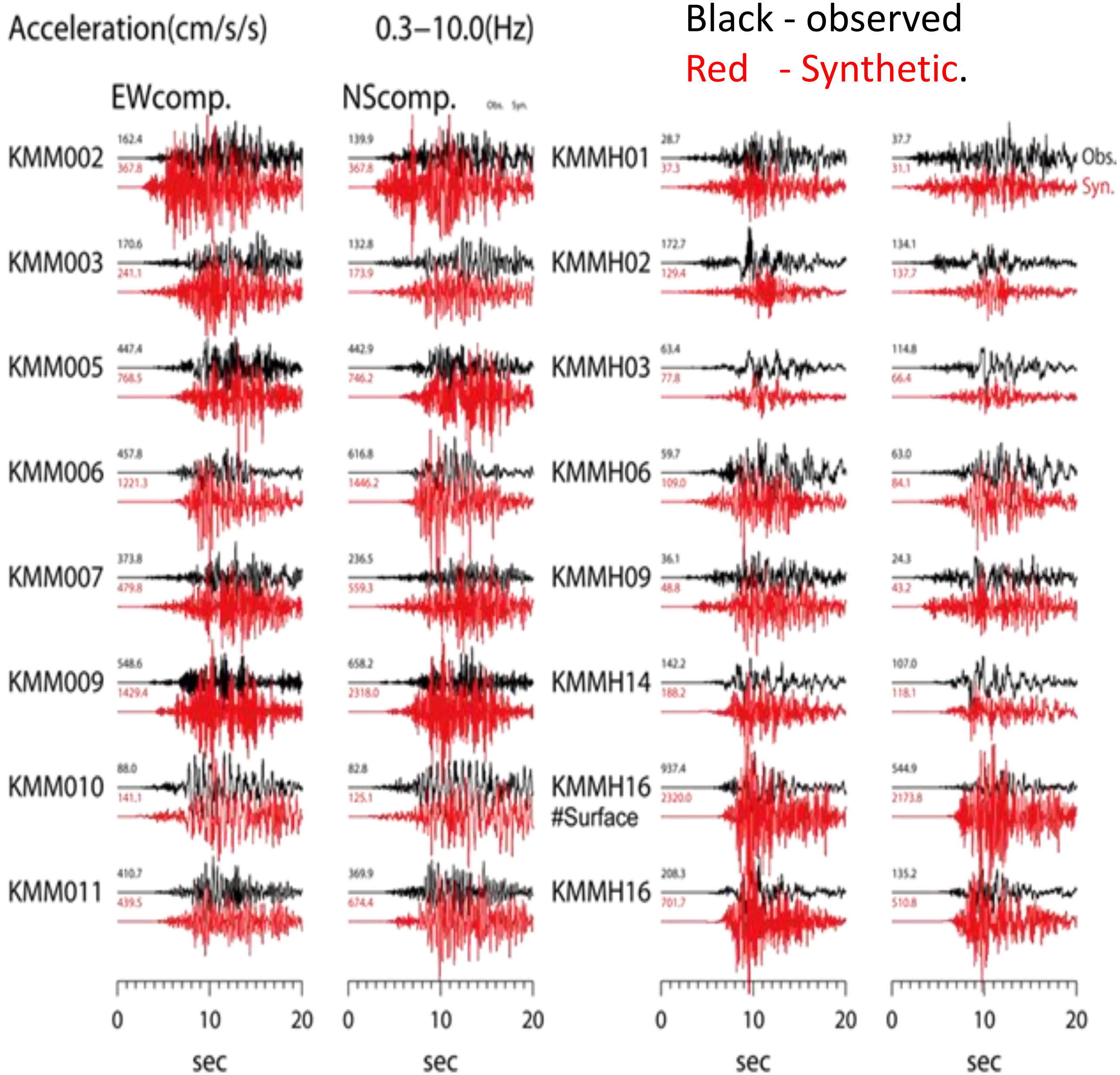

Comparison between observed and synthetic ground motions for three-SMGAs model

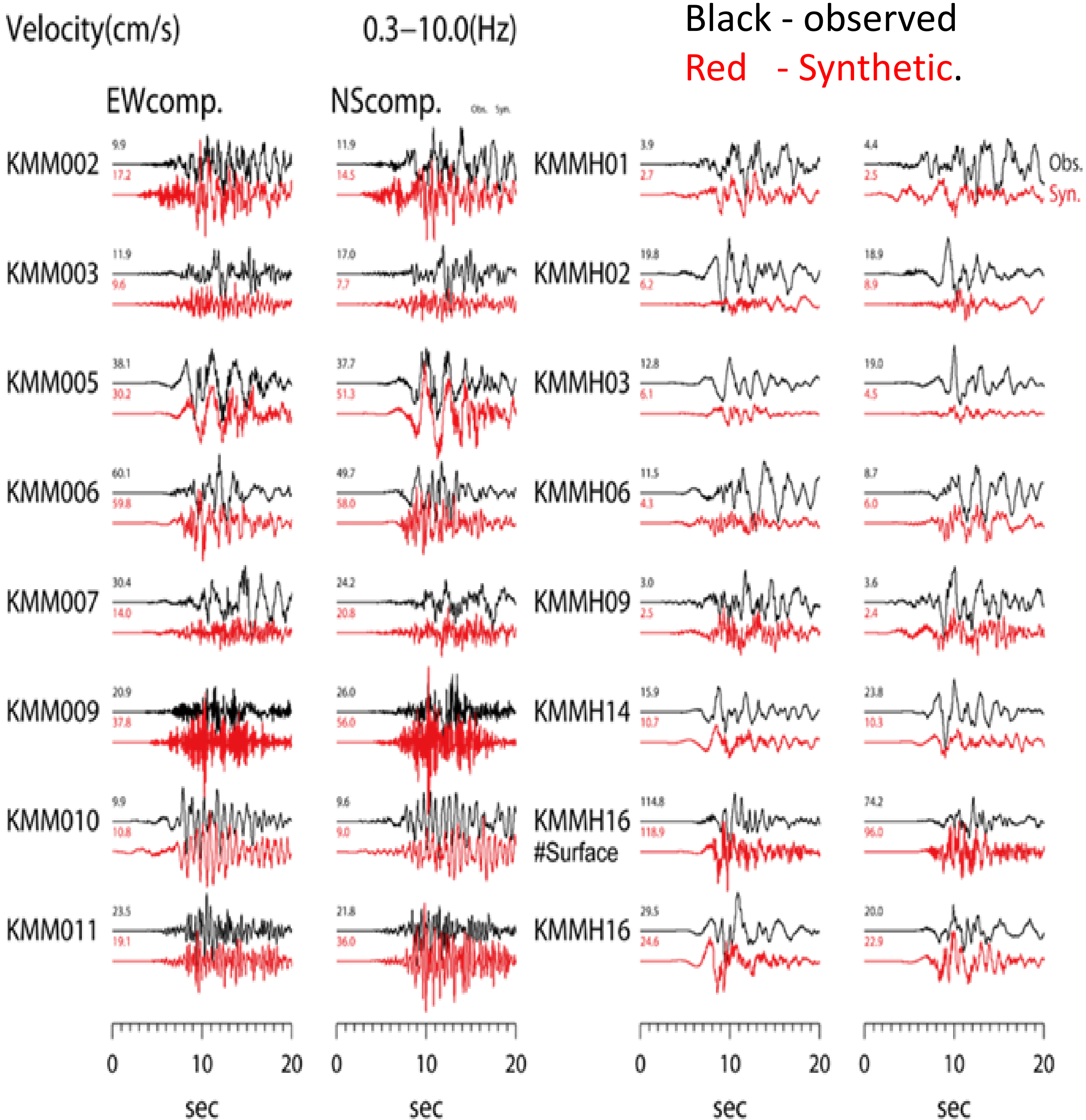

Comparison between observed and synthetic ground motions for three-SMGAs model

Black - observed

Red - Synthetic.

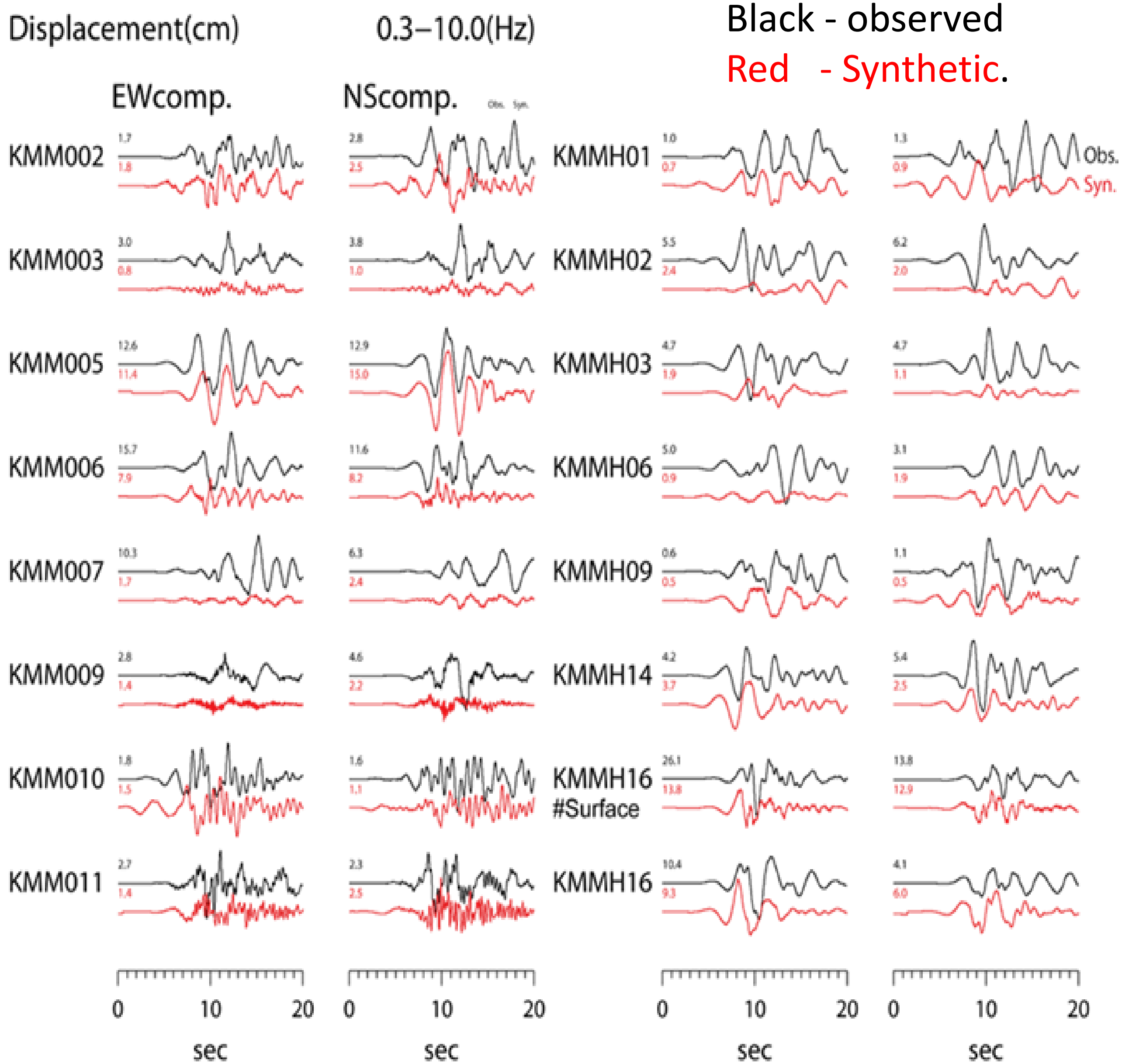

Best-fit characterized source model with a single SMGA based on the inversion result by Kubo et al. (2016)

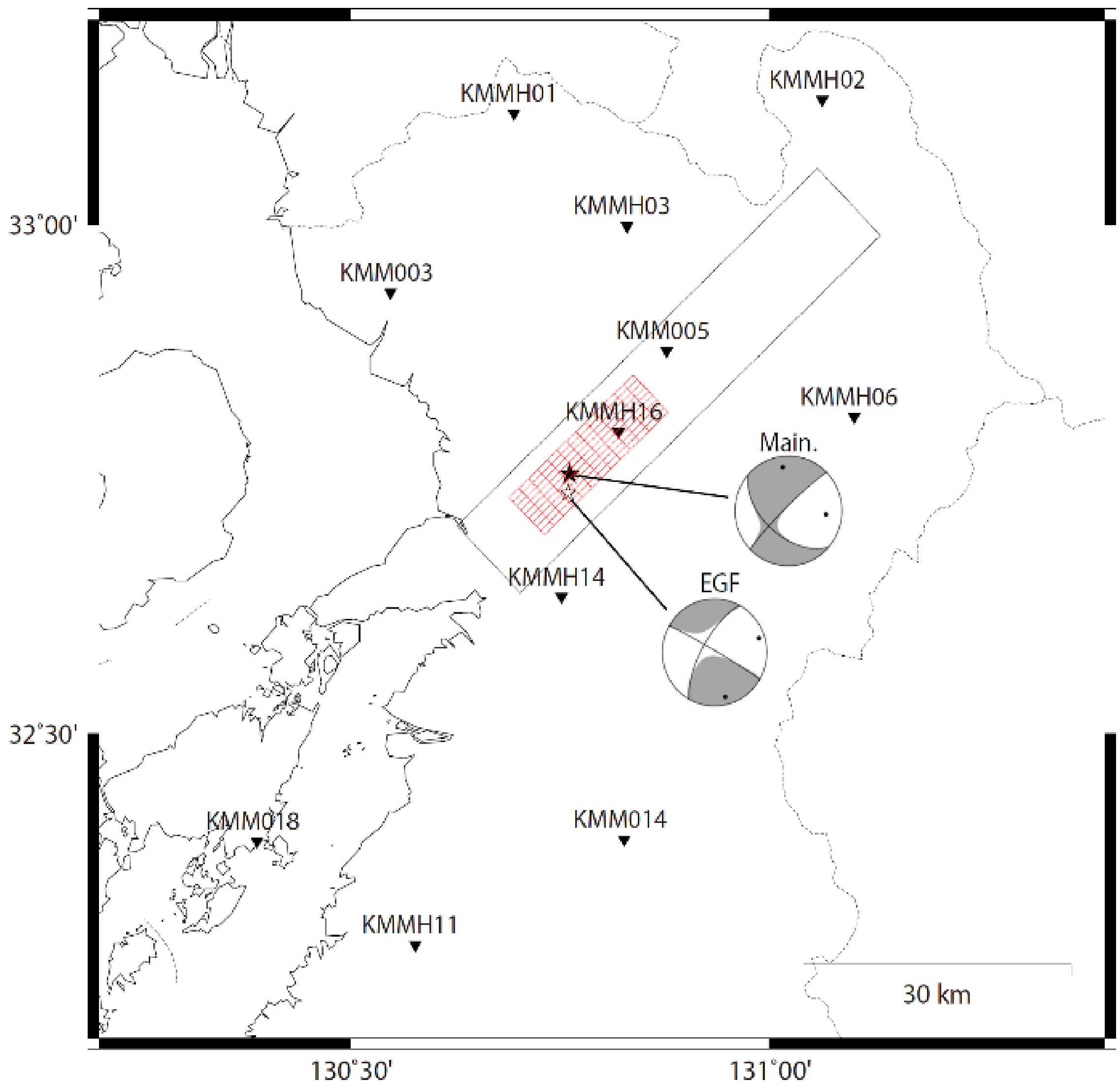

Best-fit characterized source model with a single SMGA based on the inversion result by Kubo et al. (2016)

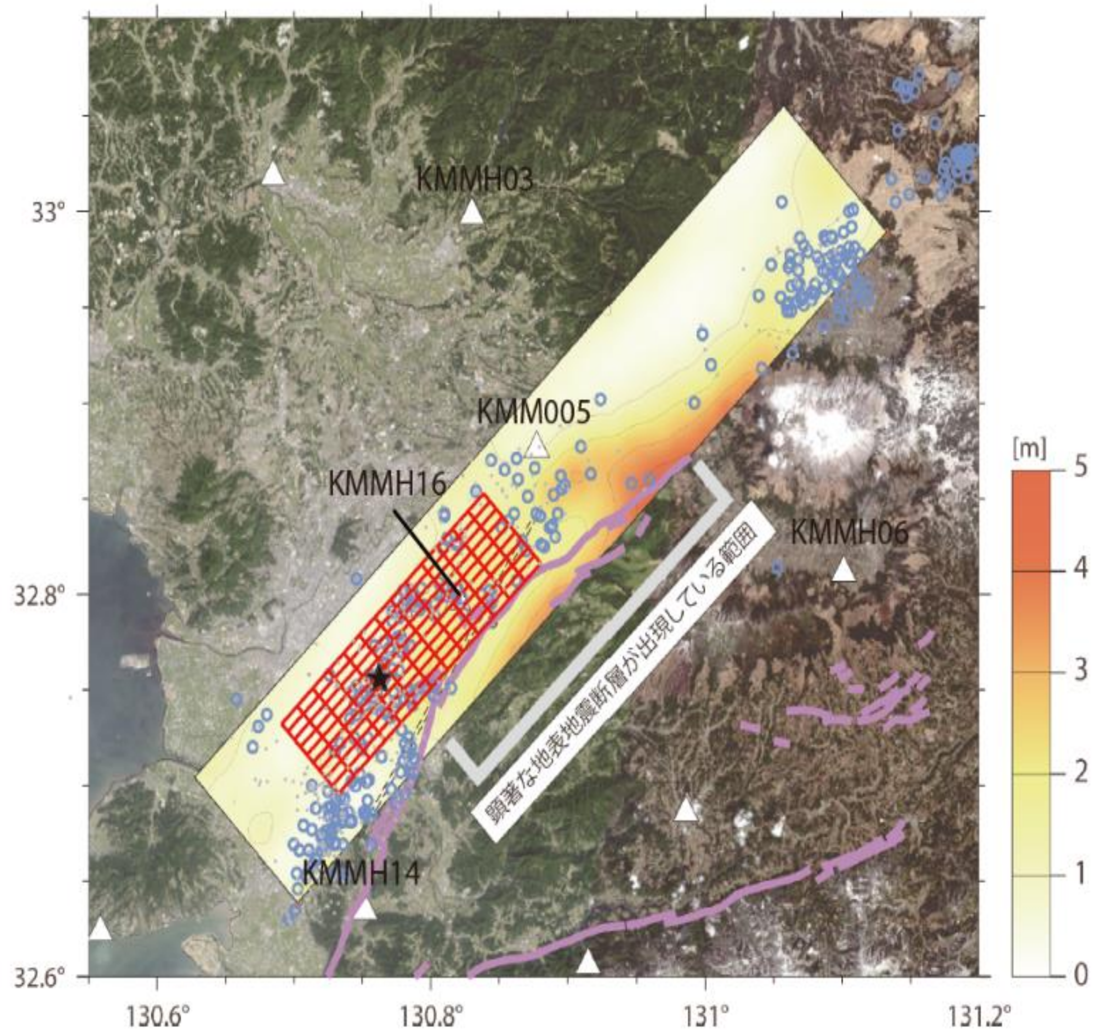

Comparison between observed and synthetic ground motions for three-SMGAs model

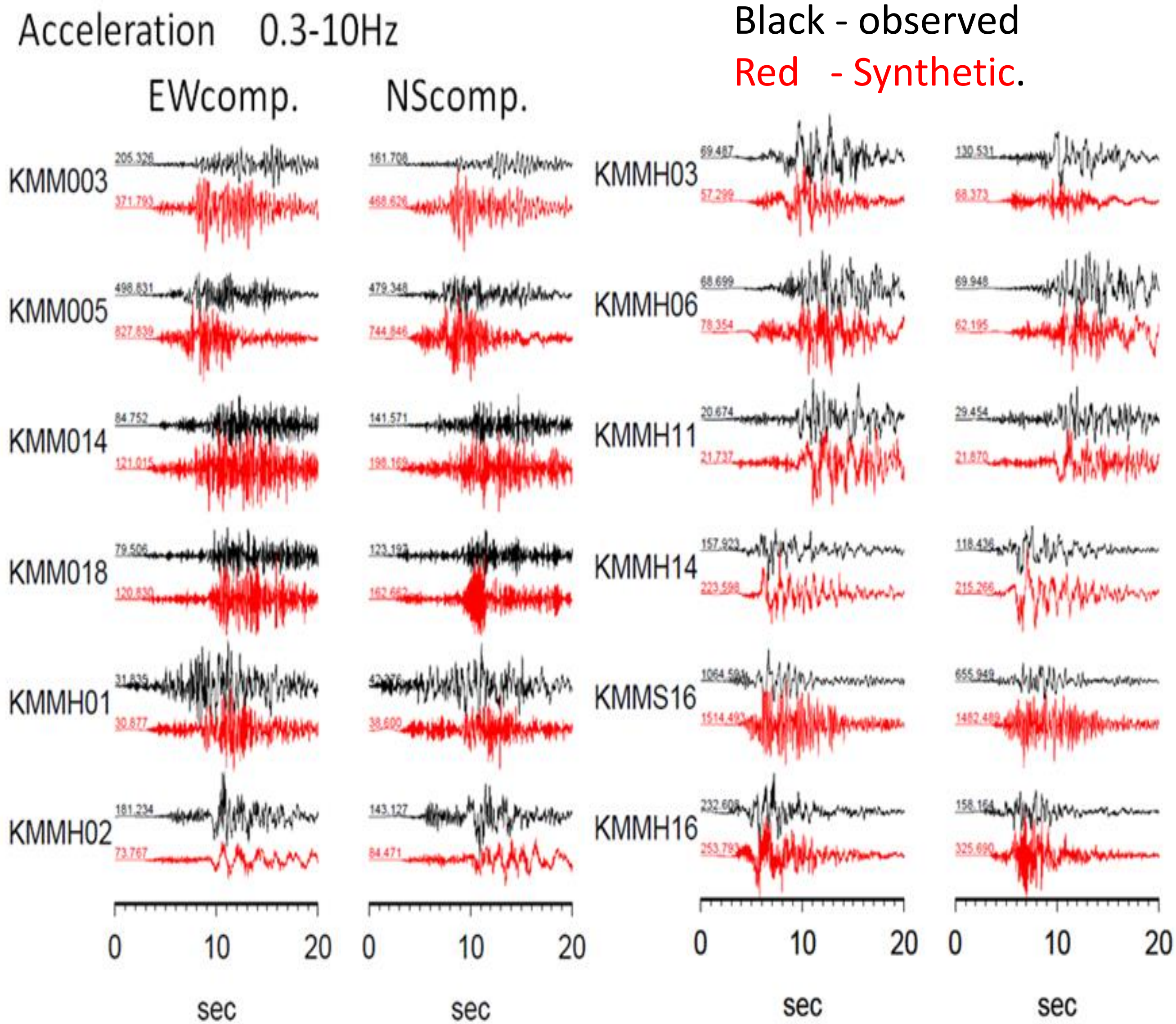

Black - observed
Red - Synthetic.

Comparison between observed and synthetic ground motions for three-SMGAs model

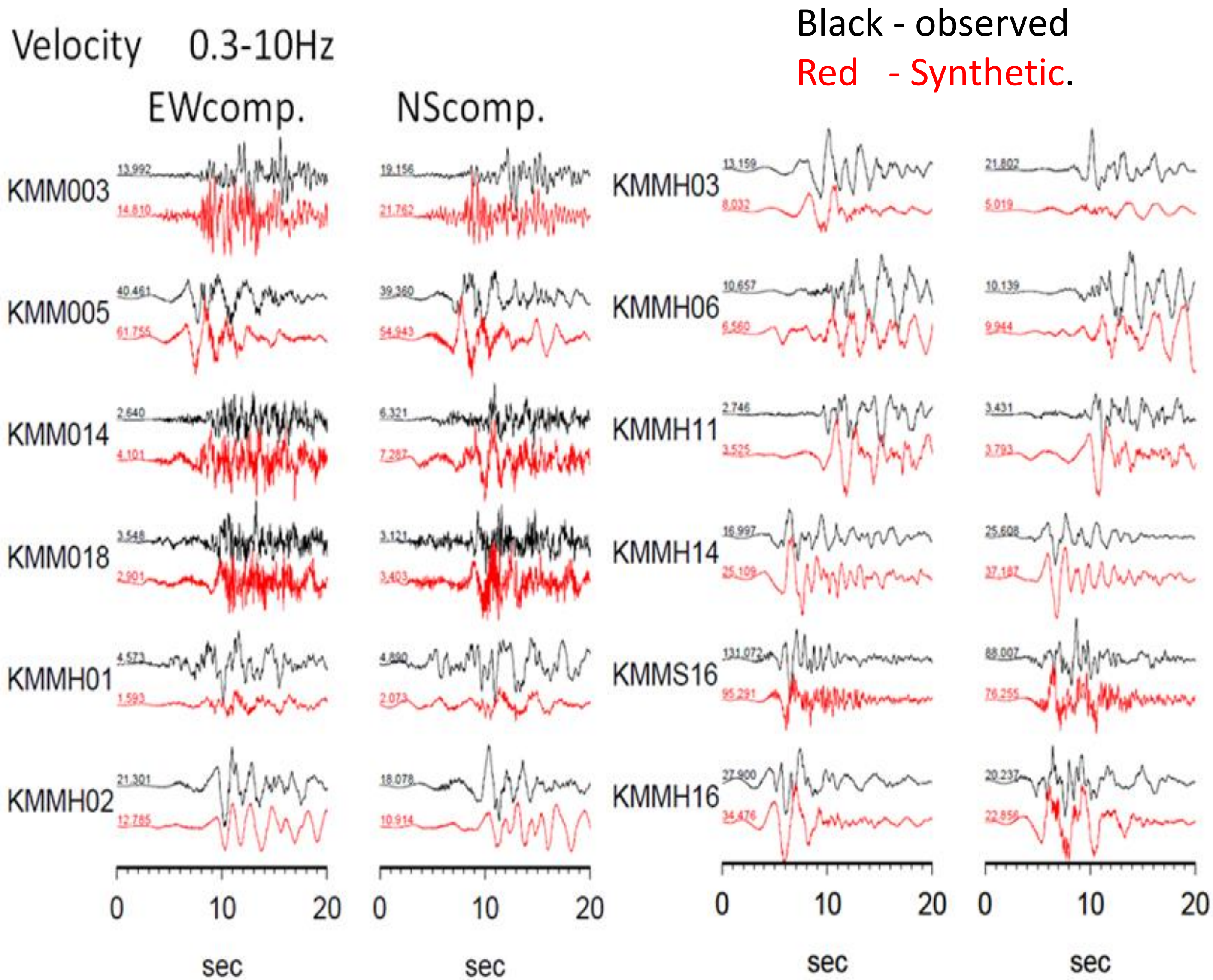

Comparison between combined area of asperities from the slip distribution and that of SMGAs from strong motion simulation

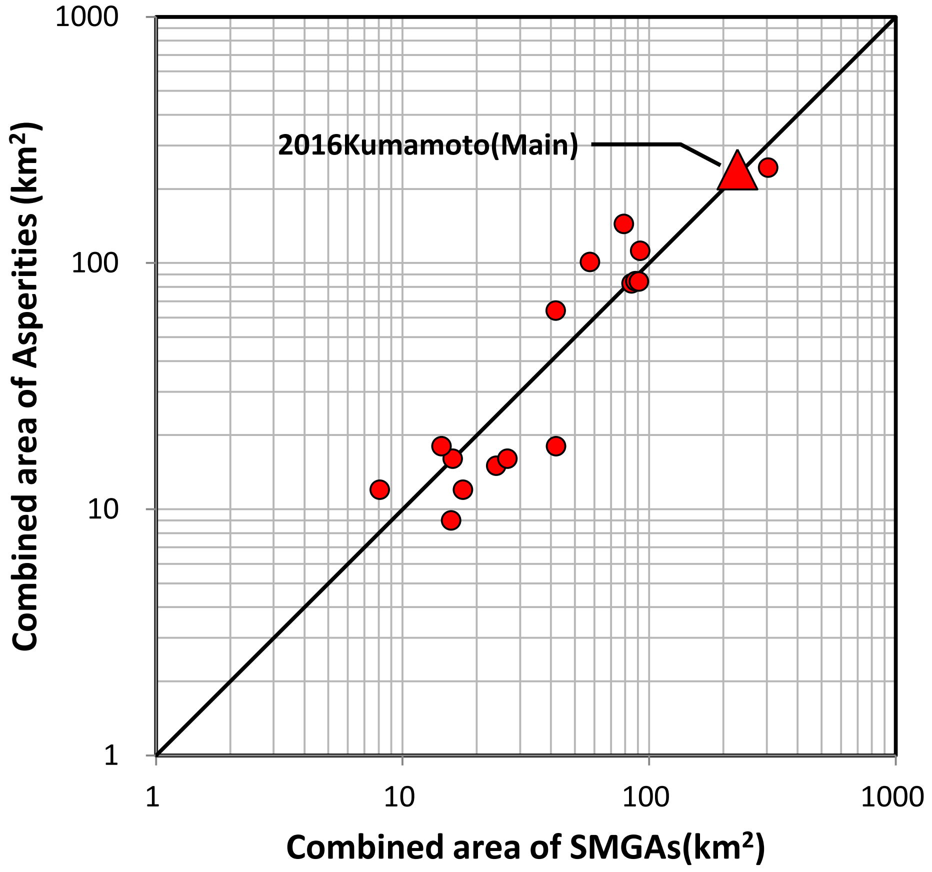

Stress parameters in combined area of asperities and in SMGAs

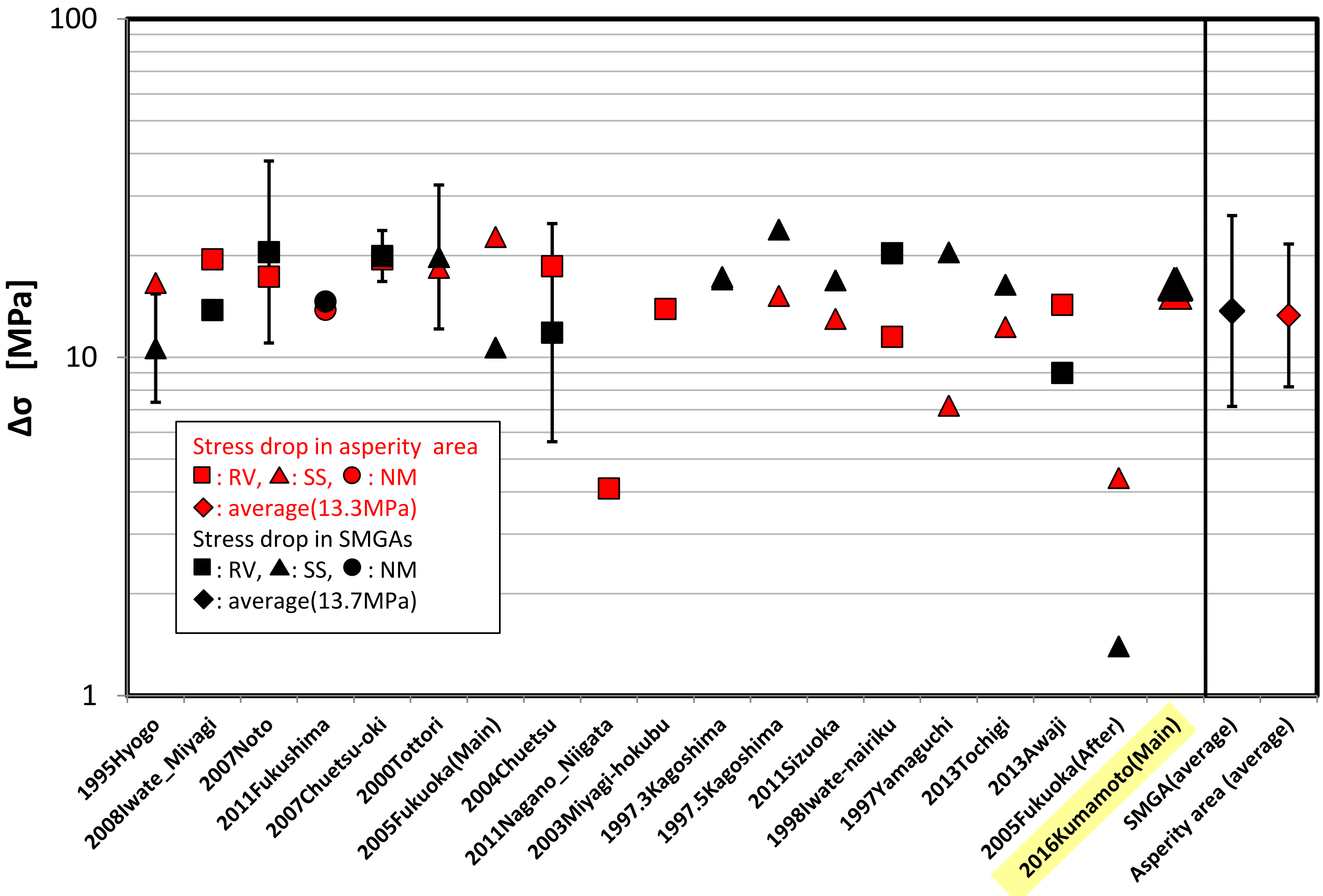

Source model of mega-thrust subduction earthquake

Rupture process of the Mw 9.0 2011 Tohoku earthquake

- Frequency-dependent rupture process: Comparison of short-period P wave backprojection images and broadband seismic rupture models (Koper et al., 2011).
- Period-dependent source rupture behavior of the 2011 Tohoku earthquake estimated by multi period-band Bayesian waveform inversion (Kubo et al., 2014)

Rupture process of other mega-thrust subduction earthquakes

- Depth-varying rupture properties of subduction zone megathrust faults such as the 2004 Sumatra-Andaman earthquake (Mw 9.2) and the 2010 Maule earthquake (Mw 8.8) (Lay et al., 2012).

Similar rupture processes are observed for recent M 8 subduction earthquakes

- Slip segmentation and slow rupture to the trench during the 2015, Mw8.3 Illapel, Chile earthquake (Melgar et al., 2015)
- Along-dip seismic radiation segmentation during the 2007 Mw 8.0 Pisco, Peru earthquake (Sufri et al., 2012)

Strong ground motion records (acceleration) near the source area of the 2011 Tohoku earthquake

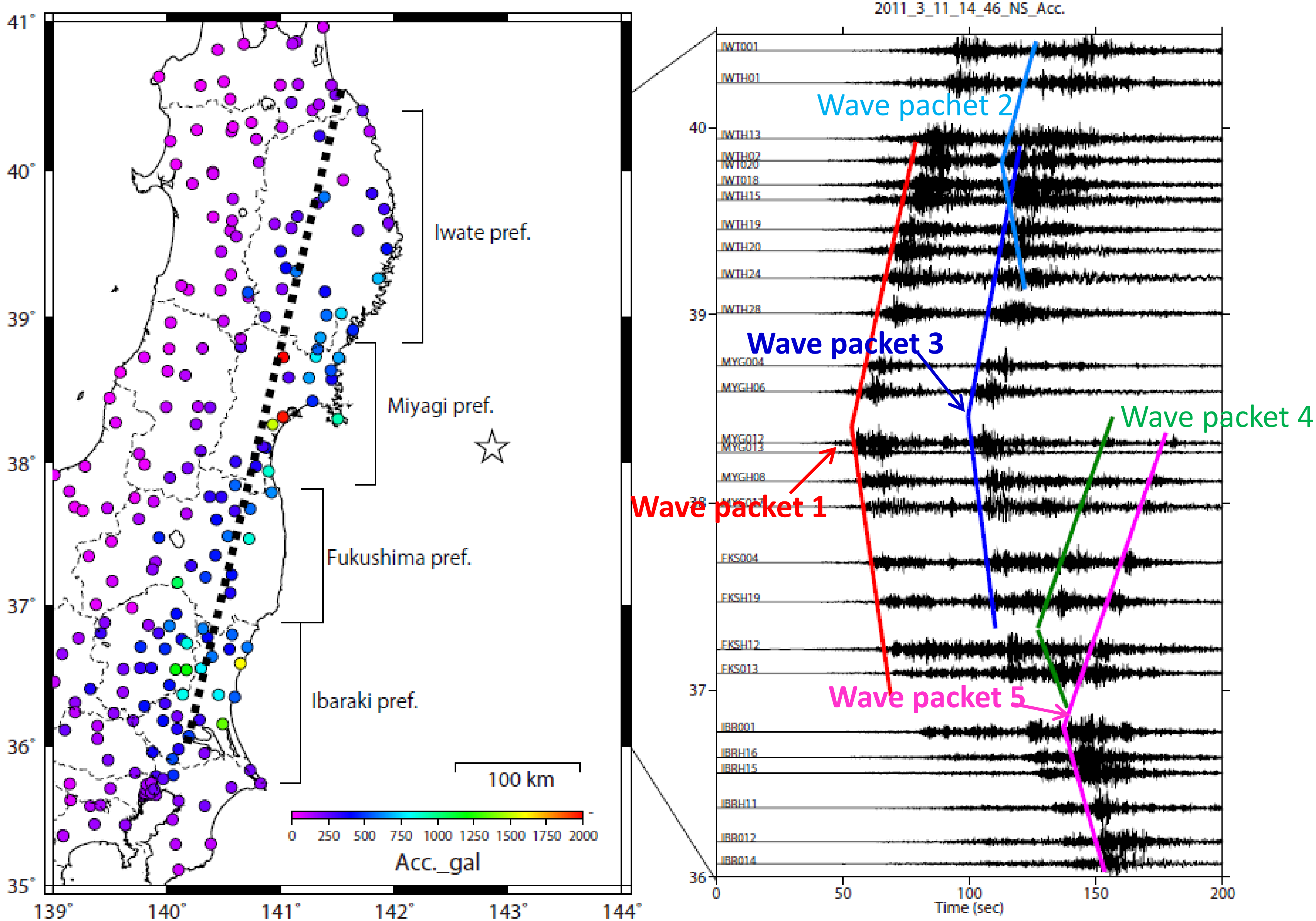

After Irikura and Kurahashi (2011)

Period-dependent source rupture behavior of 2011 Tohoku earthquake by Kubo, Asano and Iwata (2014)

Final slip distributions for each period band

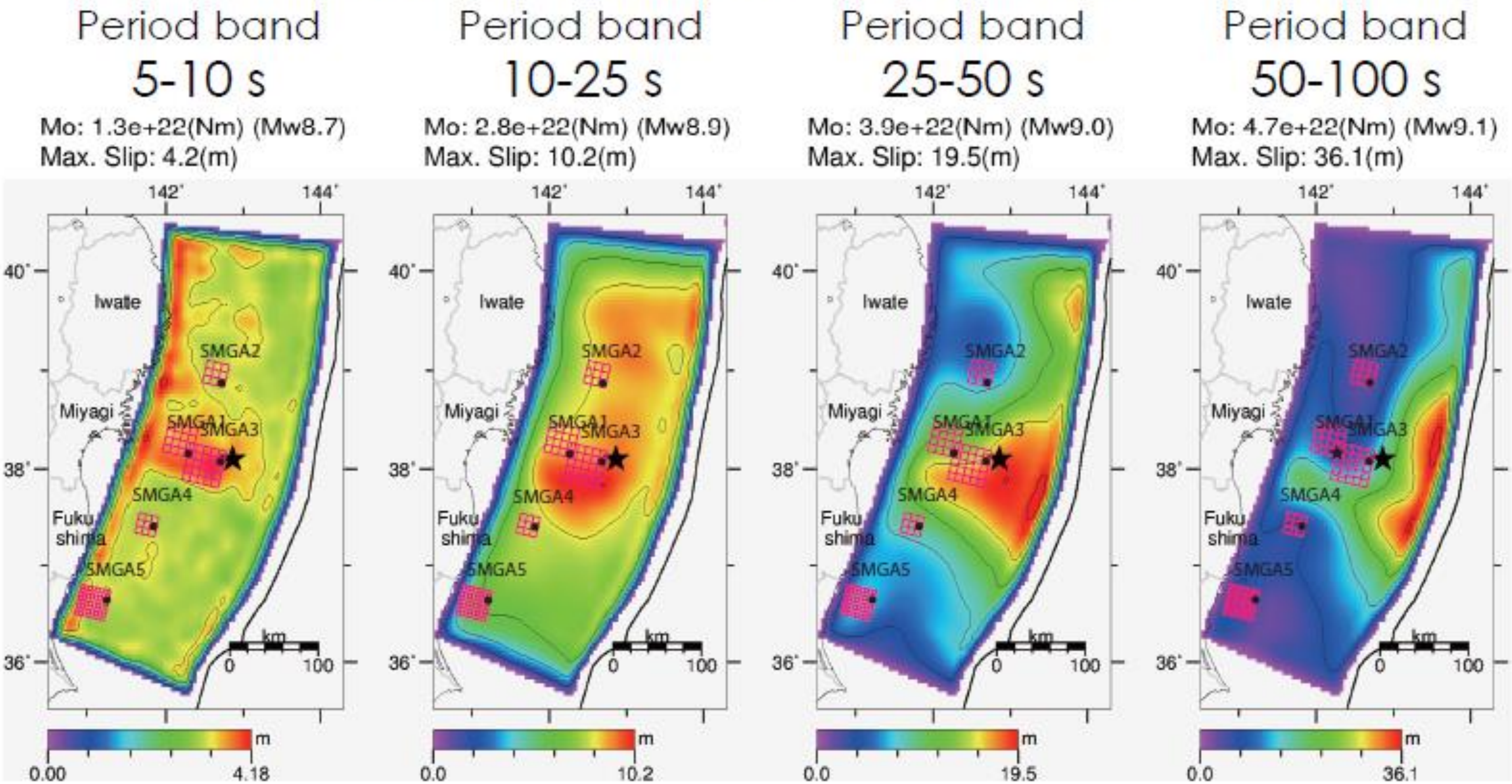

久保他(2015)に加筆

Multi-scale Heterogeneous Earthquake Model (Aochi and Ide, 2014)

Parametric Study of Multi-scale Heterogeneous Earthquake Model

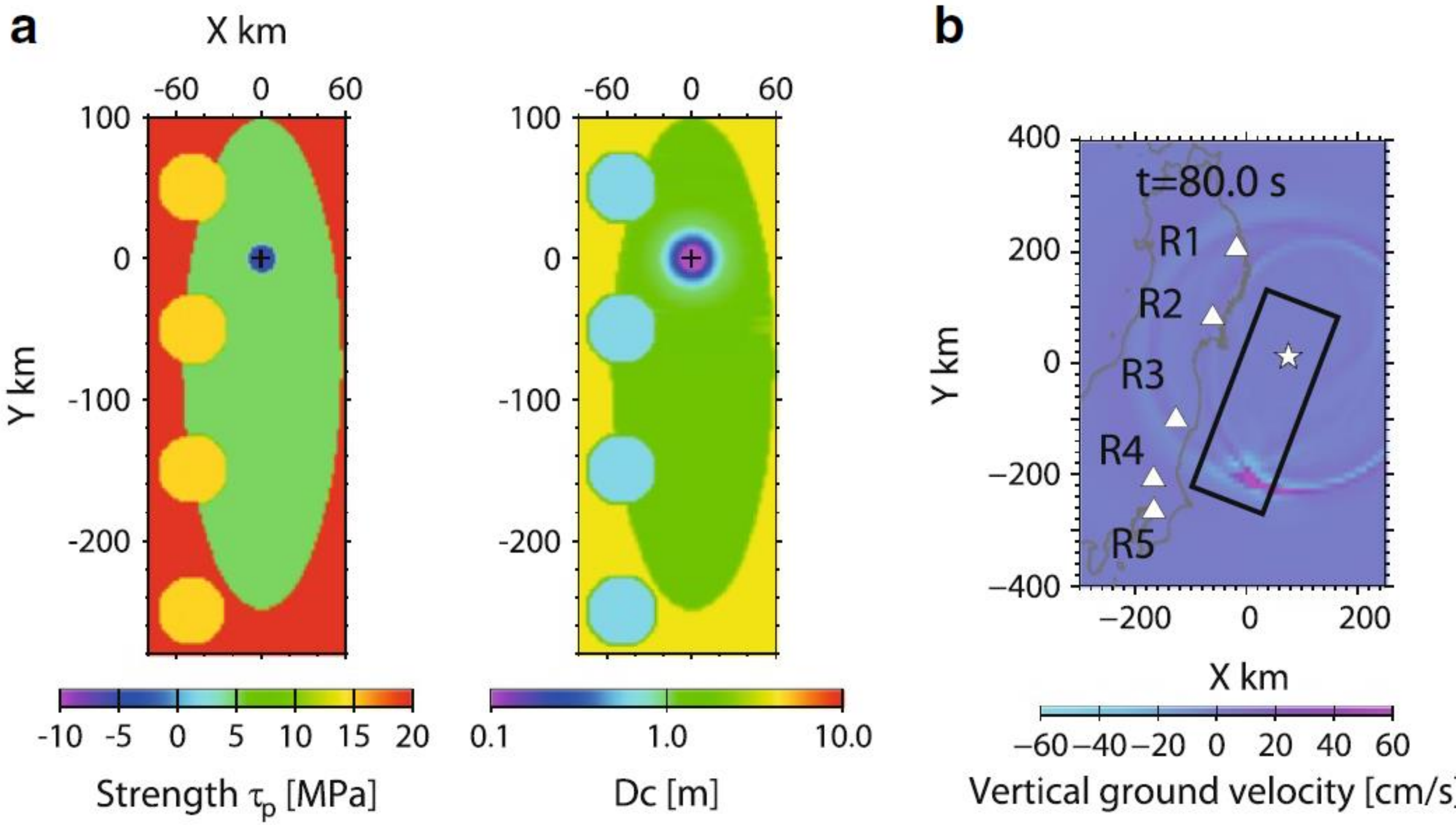

Ground motion comparison for three scenarios

(Aochi and Ide, 2014)

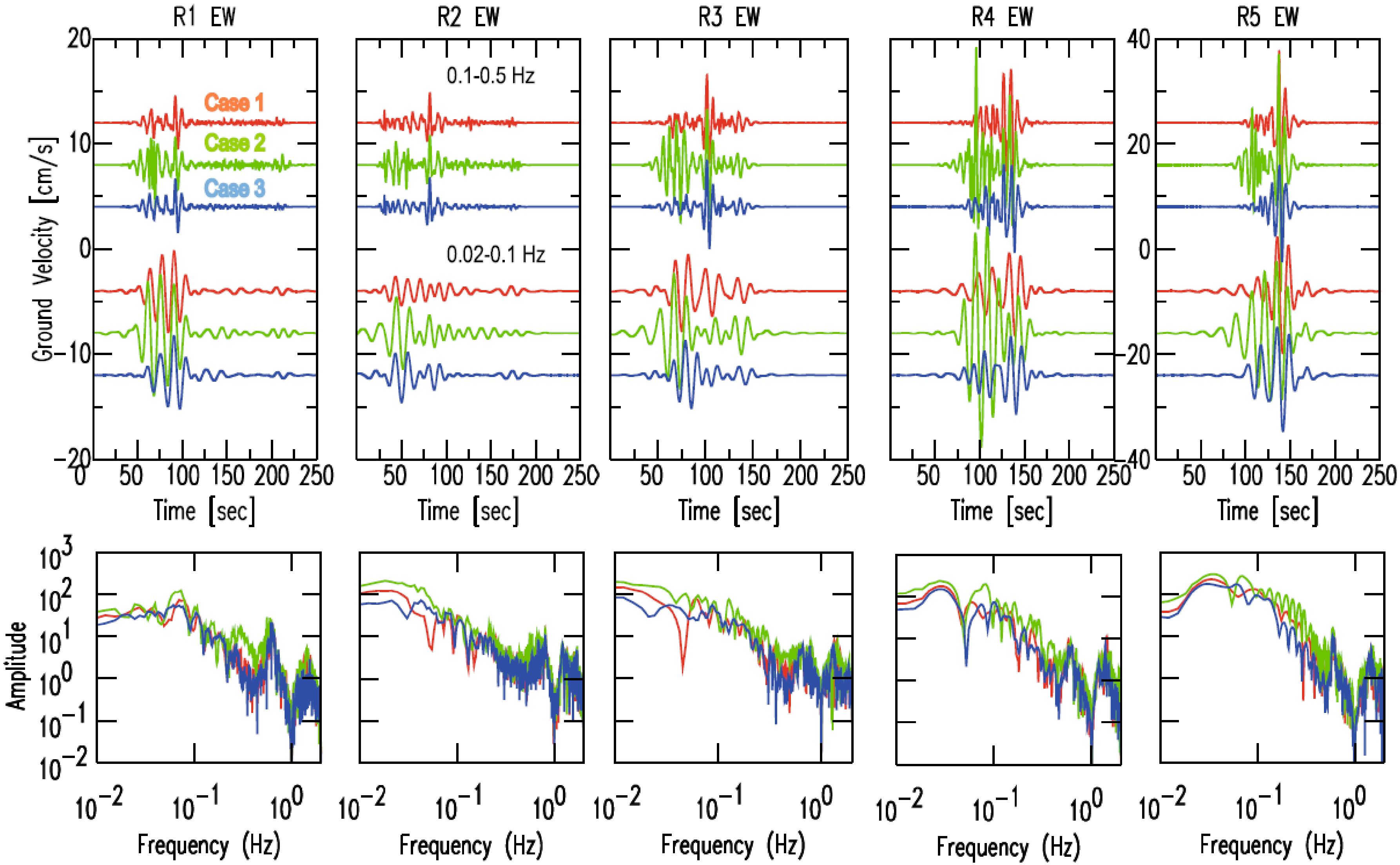

Small patchesのパラメータ	case 1	case 2	case 3
Stress excess $\Delta\tau^{excess}$ [MPa]	15	5	10
Stress drop $\Delta\tau$ [MPa]	5	15	10

An illustrative source model with multiscale heterogeneity combining tsunami and strong motion generation

(Long-Period Motion Evaluation Committee of Cabinet Office, Japan)

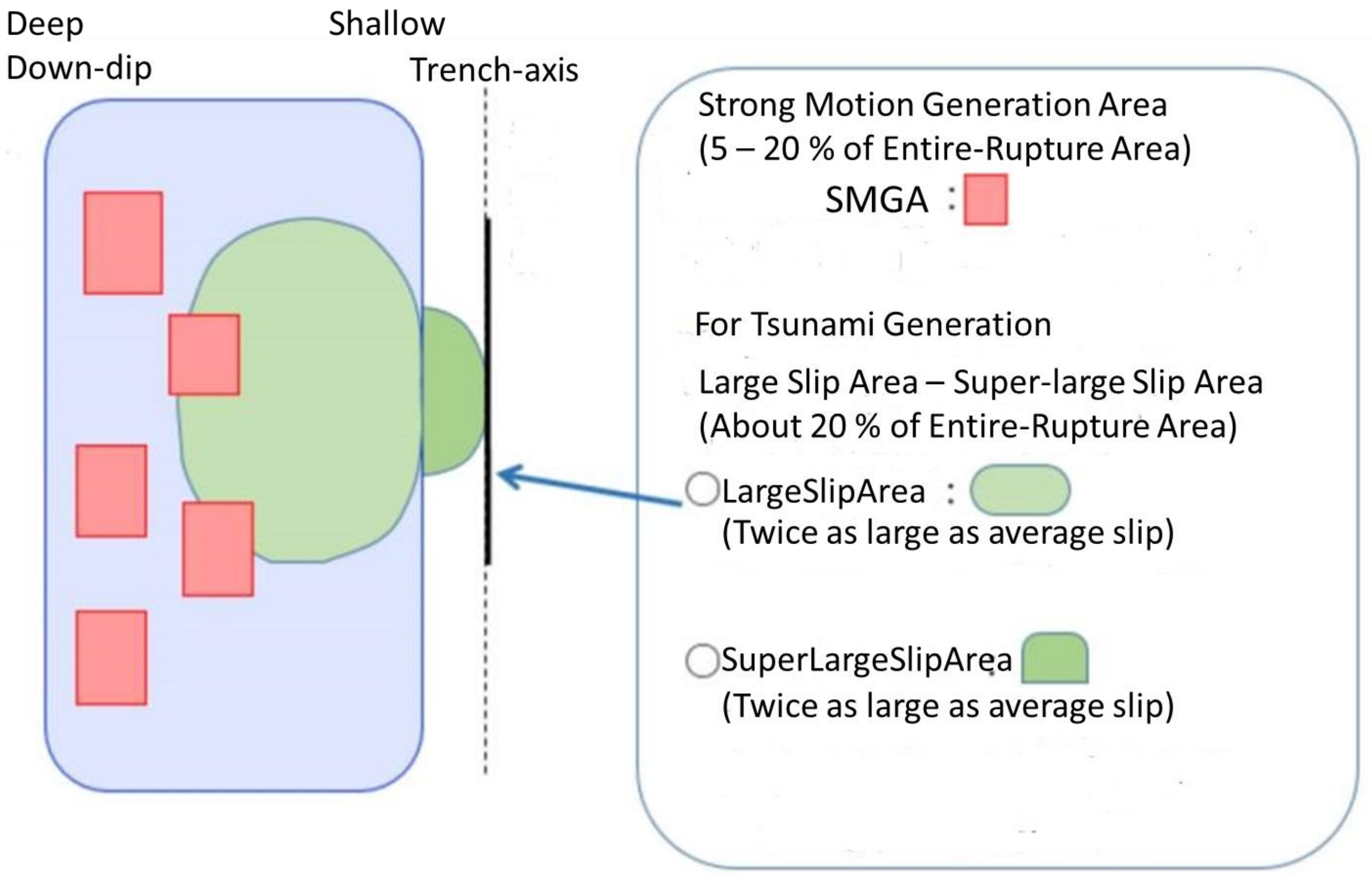

Empirical relationships between seismic moment M_o and rupture area S for subduction earthquakes

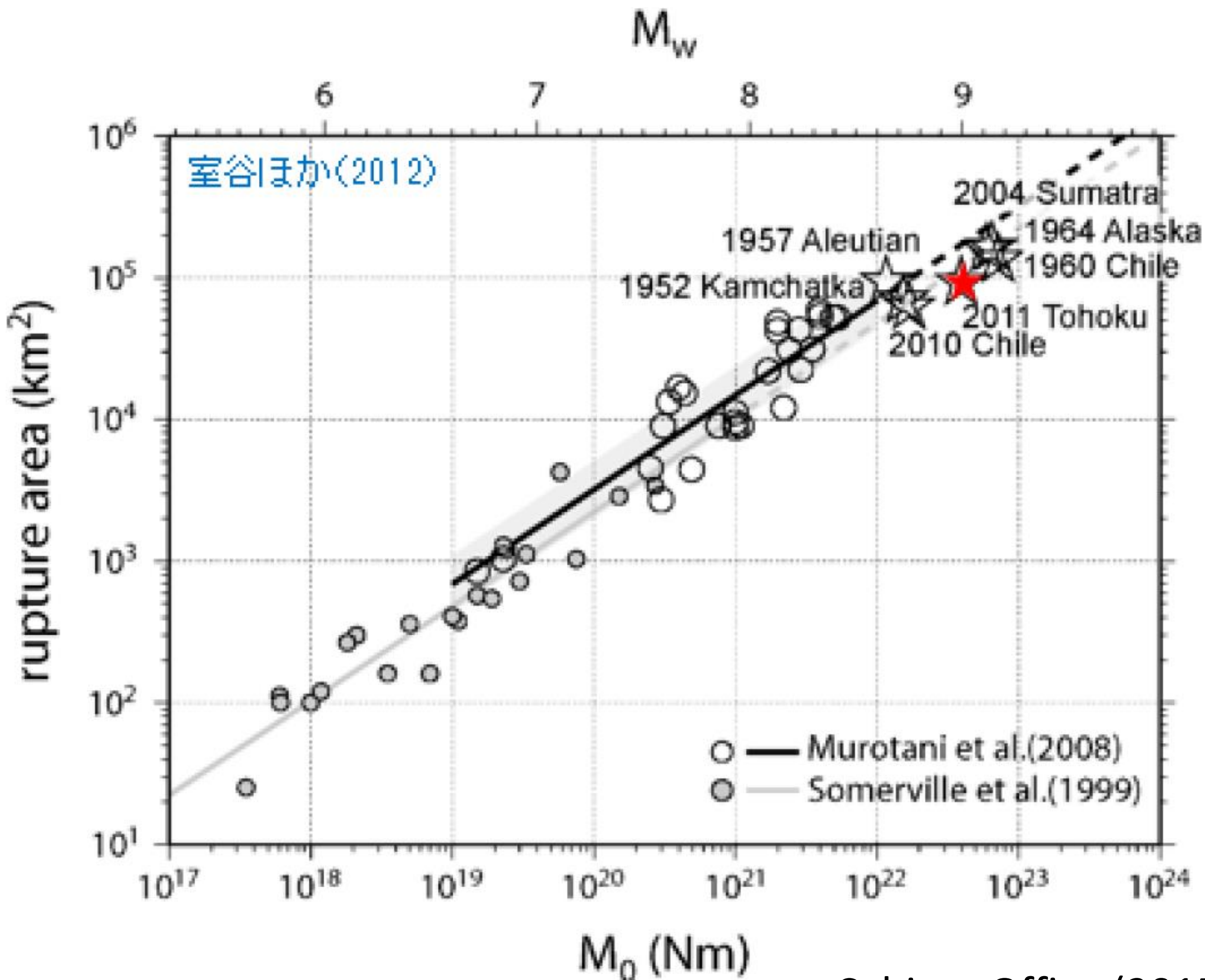

Cabinet Office (2015)

Empirical relationships between seismic moment M_o and combined area of asperities S_s for subduction earthquakes

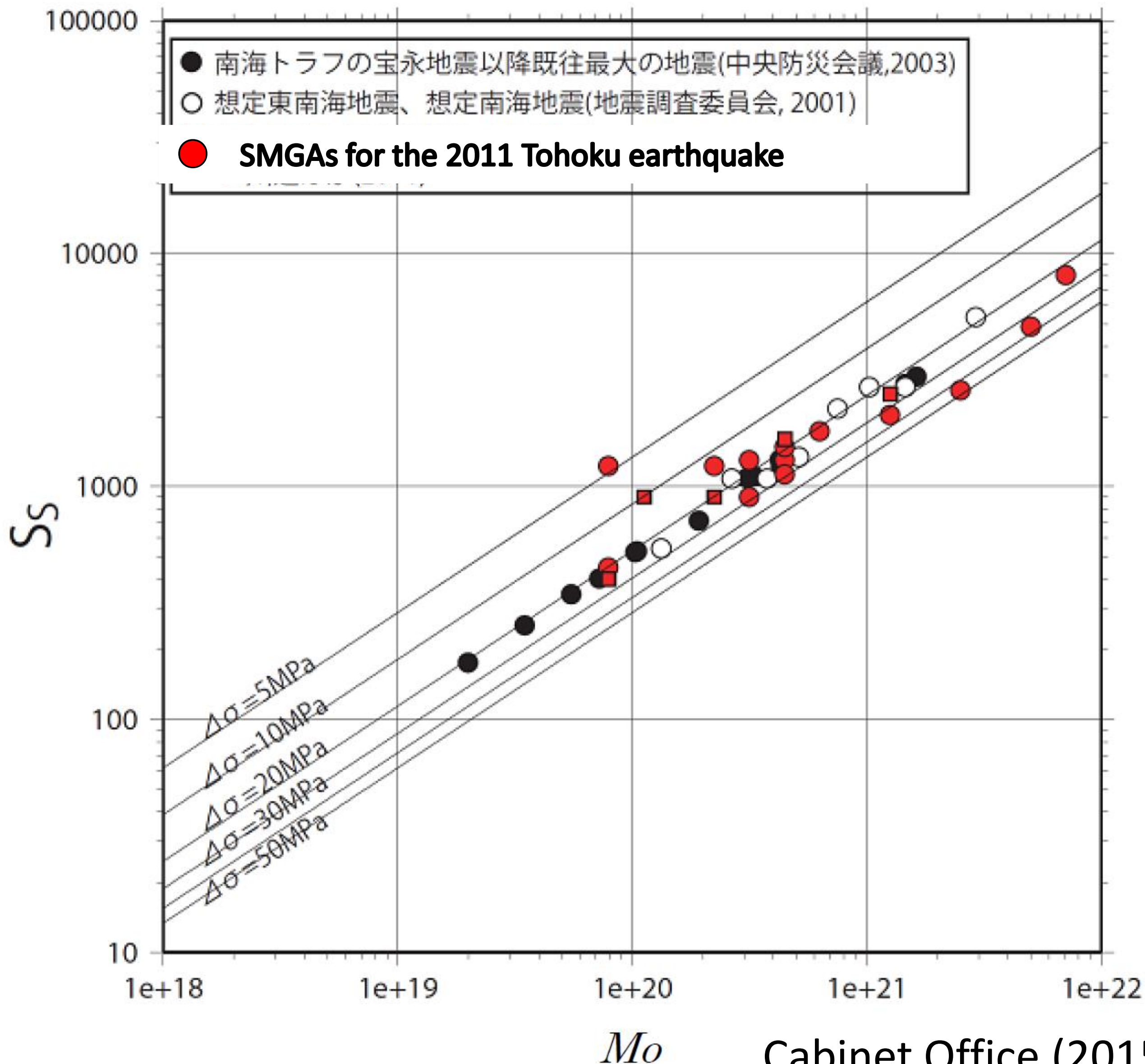

Cabinet Office (2015)

Five SMGAs' Model for the 2011 Tohoku Earthquake

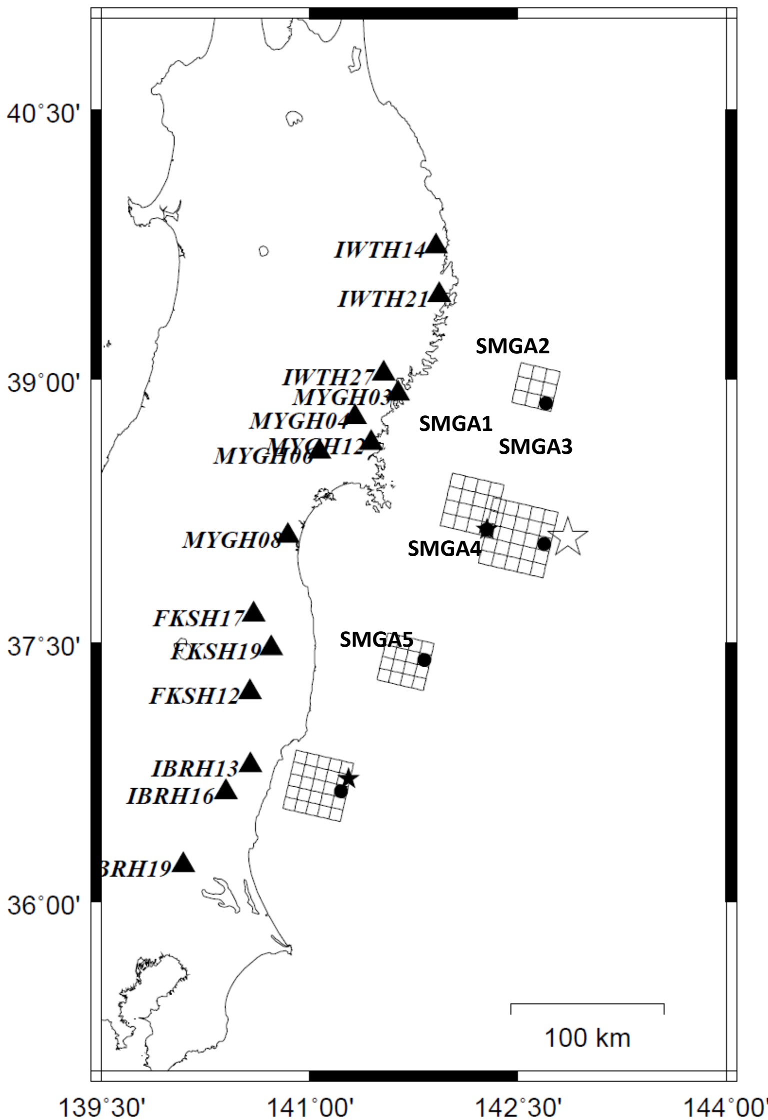

	L x W (km^2)	Mo (Nm)	Stress Drop (MPa)
SMGA1	34 × 34	2.68E+20	16
SMGA2	23.1 × 23.1	1.41E+20	20
SMGA3	42.5 × 42.5	6.54E+20	20
SMGA4	25.5 × 25.5	1.24E+20	25.2
SMGA5	38.5 × 38.5	5.75E+20	25.2

Comparison between observed and synthetic long-period motions (2 to 10 s) using numerical Green's functions for 3-D structure model

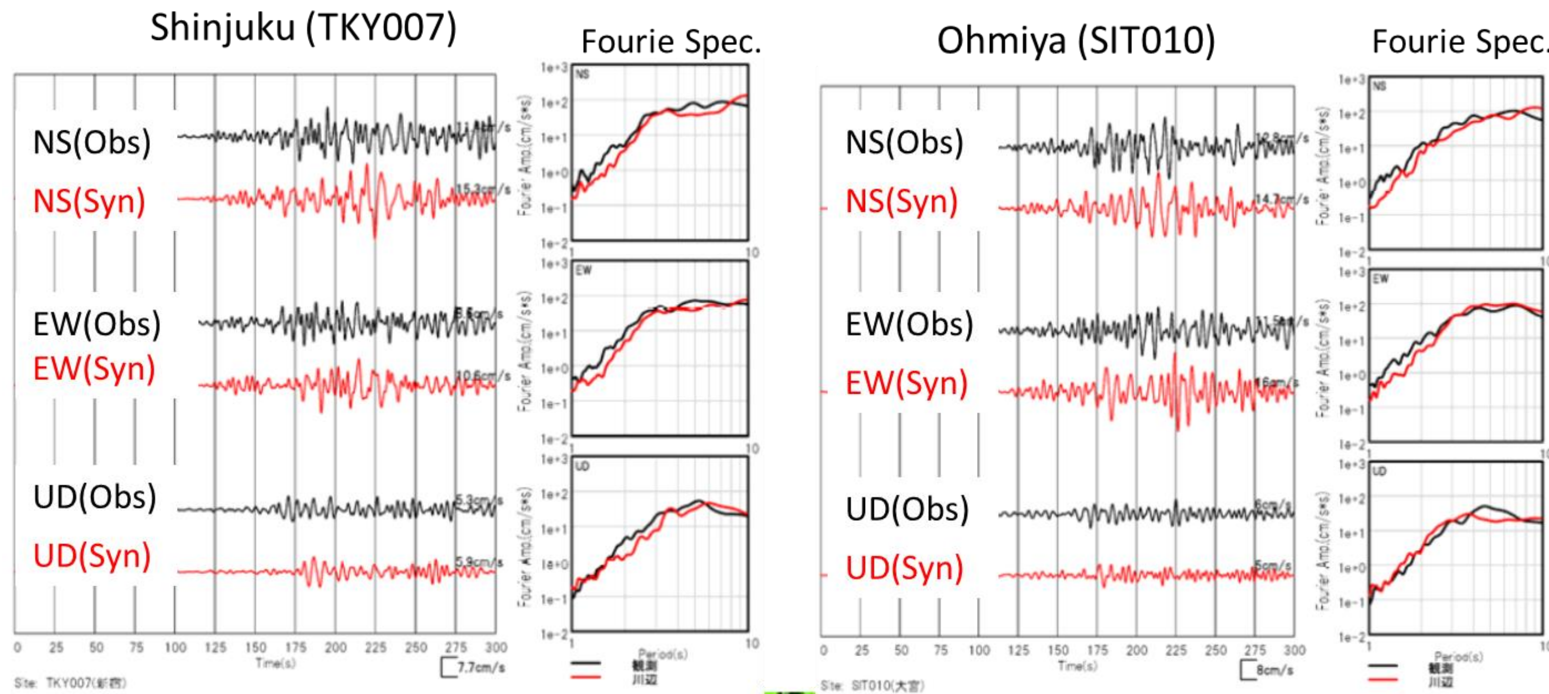

Black: observed

Red : synthetic

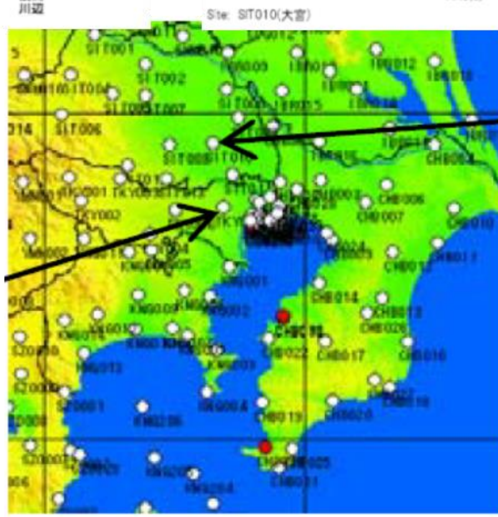

Shinjuku (TKY007)

Ohmiya (SIT010)

Cabinet Office (2015)

Comparison of Observed and Synthetics (Only SMGA1,2,3) using the empirical Green's finction method

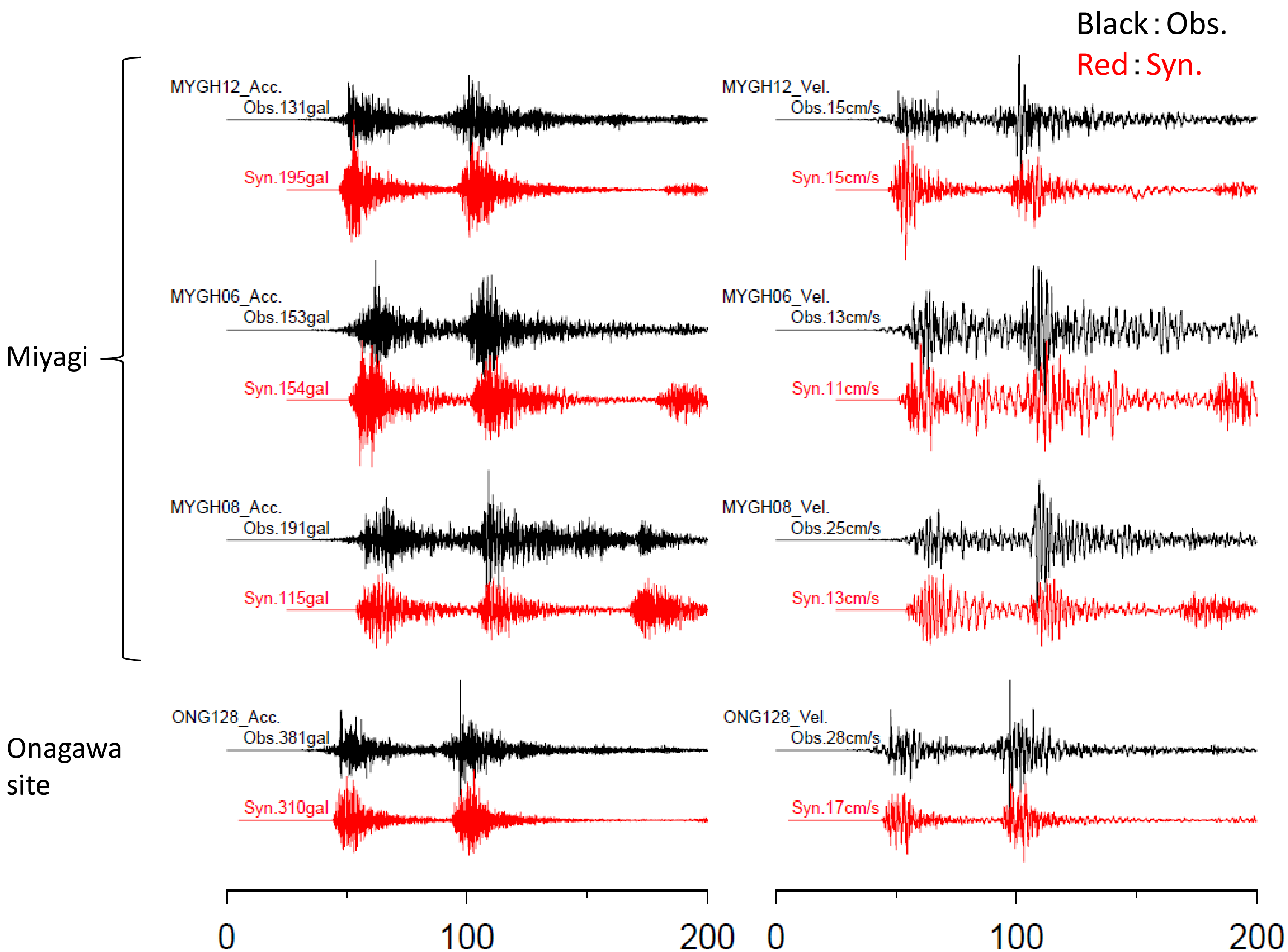

Heterogeneity inside 'strong motion generation areas' (SMGAs)

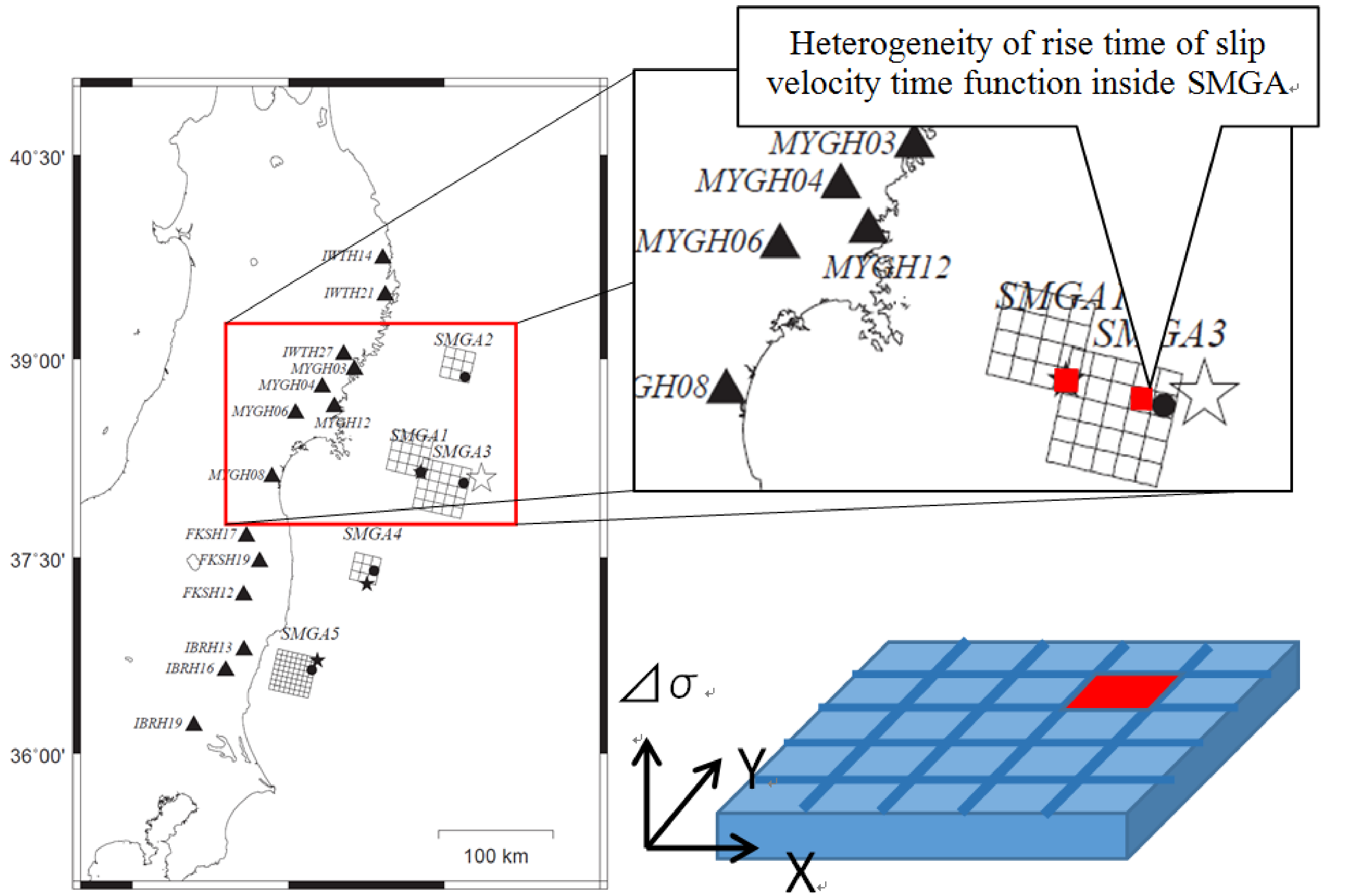

Simulated motions from a heterogeneous model, varying rise-times of slip velocity time functions at subfaults inside the SMGAs.

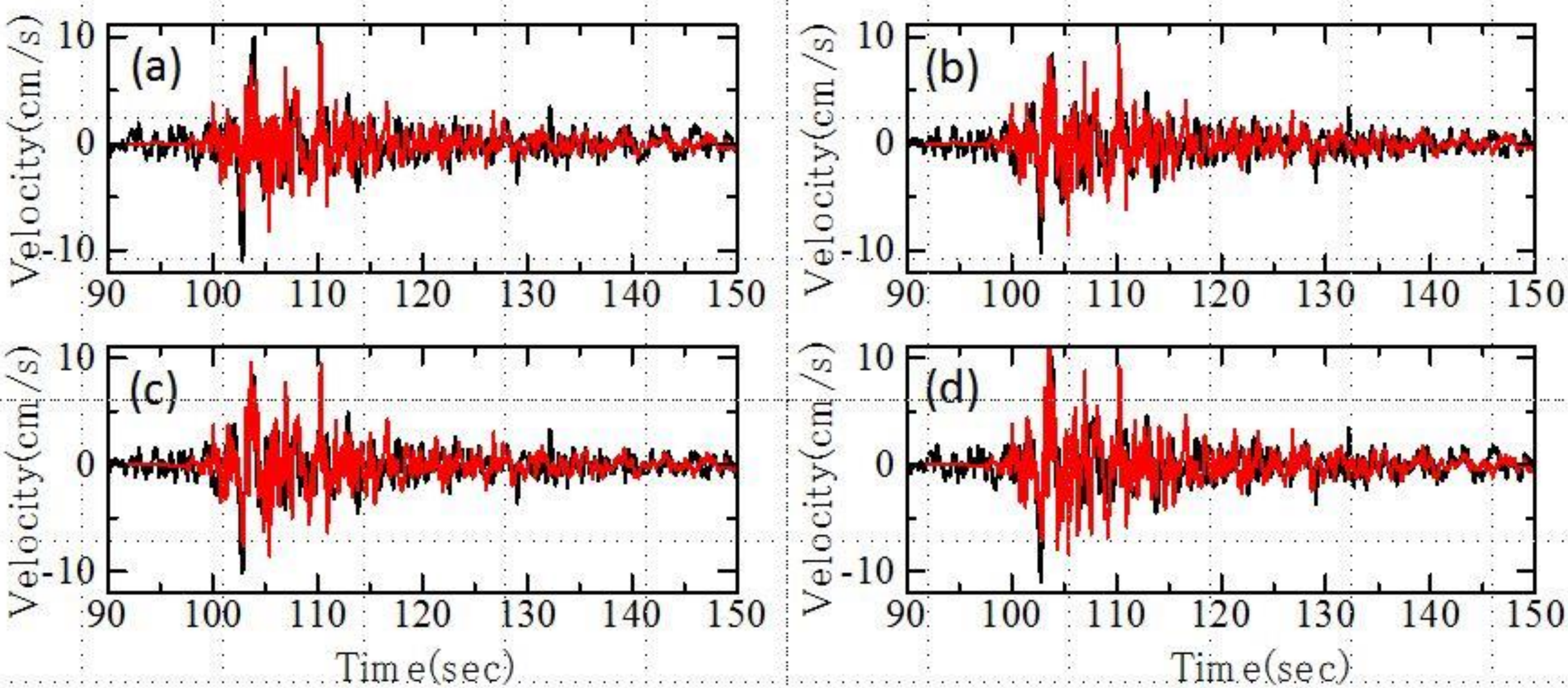

(a) Uniform model with uniform rise time of 3.7 s in all subfaults.
(b) Heterogeneous model with rise time of 2.5 s in one of the subfaults
(c) Heterogeneous model with rise time of 1.0 s in one of the subfaults
(d) Heterogeneous model with rise time of 0.25 s in one of the subfaults.

Summary of crustal earthquakes: Application to the Mw 7.0 Kumamoto earthquake

1. The source parameters estimated from the slip distribution due to the waveform inversion using strong motion data of the Mw 7.0 2016 Kumamoto earthquake follow the scaling relationship for the crustal earthquakes in Japan.

2. Strong ground motions for the 2016 Kumamoto earthquake are well simulated using the characterized model with strong motion generation areas (SMGAs).

.

Summary of mega-thrust subduction earthquakes: Application to the Mw 9.0 Tohoku earthquake

1. The observed complexity of the Mw 9.0 2011 Tohoku-Oki earthquake such as period-dependent source rupture behavior may be explained by such heterogeneities with fractal patches (size and number) by Aochi and Ide (2014).
2. Synthetic ground motions from the SMGAs match well the observed ones in long-period (2 to 10 s) range as well as those in short-period range (0.1 to 2 s) at most of stations as long as velocity structures in target areas are estimated.

Source-Fault Model for Simulation

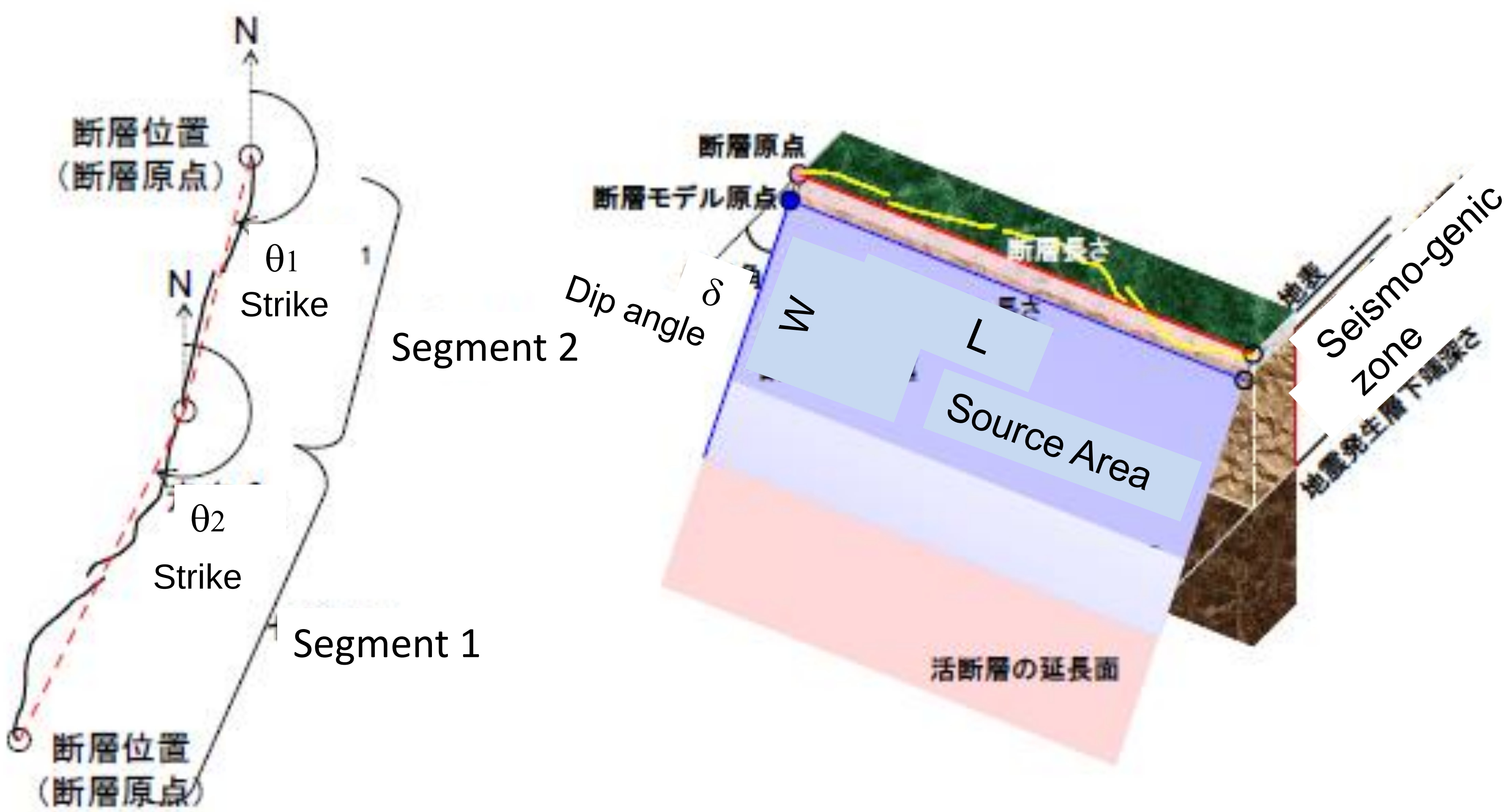

Outer Fault Parameters

Parameters characterizing entire source area

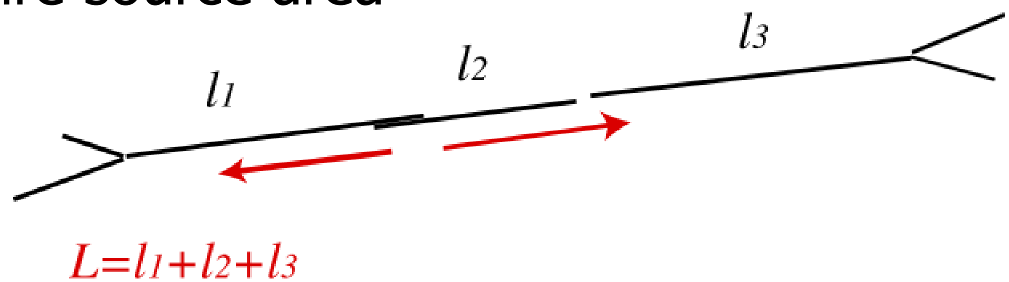

Inland crustal earthquake

- **Step 1**: Give total rupture area ($S=LW$)
  - Fault length (L) is related to grouping of active faults from geological and geomophological survey.
  - Fault width (W) is related to thickness of seismogenic zones (Hs) and dip (θ), *i.e.* $W=Hs/\sin\theta$.
- **Step 2**: Estimate total seismic moment (Mo)
  empirical relationships
- **Step 3**: Estimate average static stress-drop ($\Delta\sigma_c$) on the fault
  a circular-crack model (Eshelby, 1957) for L/W less than 2
  or a loading model (Fujii and Matsu'ura, 2000) for L/W more than 2.

Inner Fault Parameters

Slip heterogeneity or roughness of faulting

<u>Inland crustal earthquake</u>

- Step 4: Estimate combined area of asperities (Sa) from empirical relation Sa-S
  (Somerville et al., 1999; Irikura and Miyake, 2001 →)

  Sa: combined area of asperities (inner)

  S : total rupture area (outer)

  Sa/S = const (0.22 to 0.16)
  depending on regions.

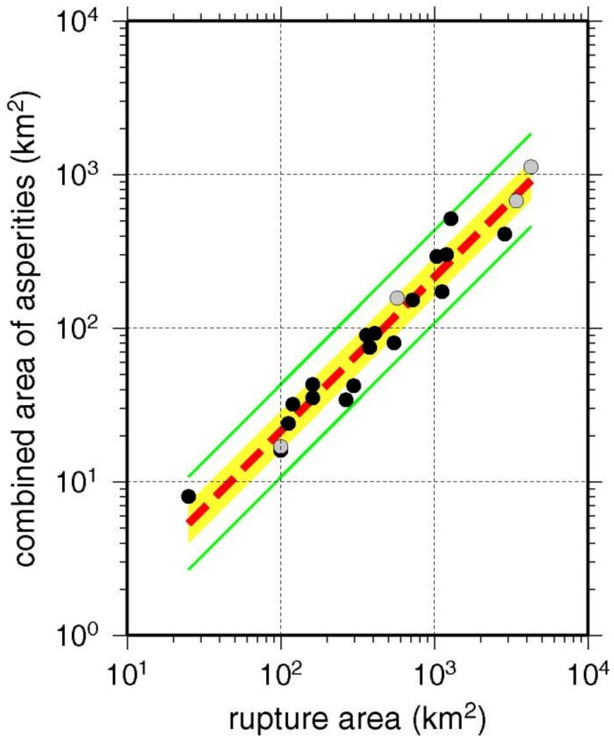

– Step 5: Estimate Stress Drop on Asperities ($\Delta\sigma_a$) from multi-asperity model (Madariaga, 1979)

$$\Delta\sigma_a = \Delta\overline{\sigma}_c \cdot \frac{S}{S_a}$$

$\Delta\sigma_a$: stress drop on asperity (inner)

$\Delta\sigma_c$: average stress drop (outer)

Inner Fault Parameters –continued 1-

Slip heterogeneity or roughness of faulting

Inland crustal earthquake

Alternative

- Step 4: Evaluate acceleration source spectral level from entire fault (Ao) using the records of past earthquakes

  Reference: Empirical relationship of Mo-Ao →

- Step 5: Assuming Ao～Ao$_a$, estimate Asperity area (Sa) from theoretical representation of Ao$_a$, Mo, and S

$$\frac{A_0^b}{A_0^a} = \sqrt{\frac{S_b}{S_a}} \cdot \frac{\sigma_b}{\sigma_a} << 1 \quad \therefore \quad \frac{A_0^a}{A_0} = \frac{1}{\sqrt{1+\left(A_0^b / A_0^a\right)^2}} \approx 1$$

$$\boxed{S_a = \left(\frac{7\pi^2}{4}\beta v_r\right)^2 \cdot \frac{(M_0)^2}{S(A_0{}^a)^2}}$$

(Sa = 722.4 km^2)

Empirical relationship shows Ao∝Mo$^{1/3}$(Dan et al., 2001)